



ECORD  IODP-Italia

**Unlocking the secrets of slow slip events:  
the role of lithological and geometric  
heterogeneity of the subducting plate**

**FRANCESCA MENEHINI**  
*(and many others!)*



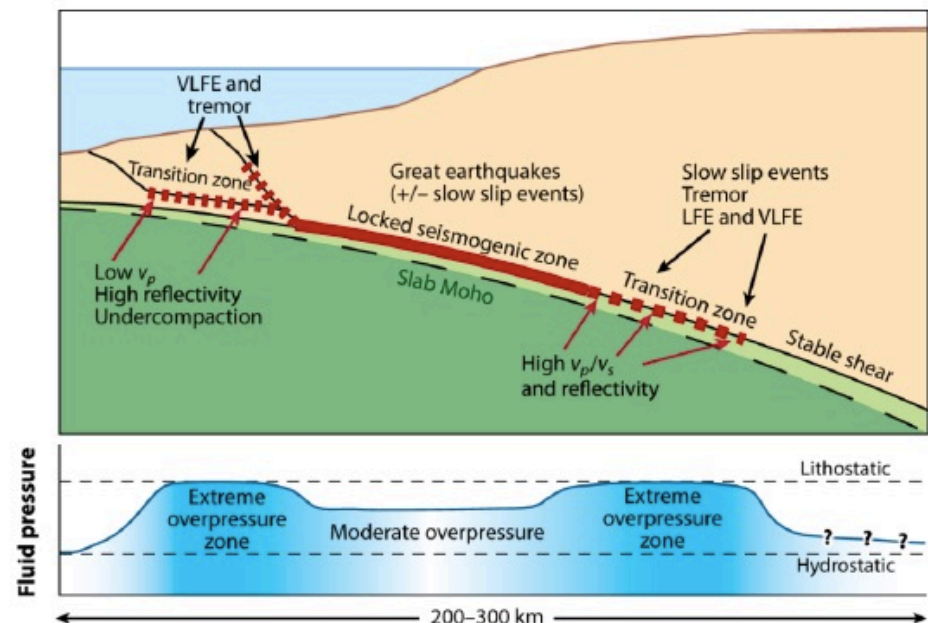
DIPARTIMENTO DI SCIENZE DELLA TERRA  
UNIVERSITÀ DI PISA

Crustal fault zones (comprising subduction thrusts ) accommodate displacement in a variety of slip styles:

- steady creep at rate typical of plate motions (1-10 cm/y);
- coseismic slip at rate ca. 1 m/s: nearly all of  $M_w > 8$  earthquakes occur along the seismically active part of the subduction plate interface thrusts;
- everything in between falls in the category of **slow earthquakes**, a category of slip events with durations up to several orders of magnitude longer than regular earthquakes of comparable size (slow slip events (SSEs), tremor and low-frequency earthquakes) - see Kirkpatrick et al., 2021

### WHAT ARE SSEs?

- transient aseismic slip on a fault lasting for days to years
- slip velocities too small to radiate seismic energy and cause ground shaking
- recorded both at the upper and lower transitions to aseismic slip along the plate interface (associated with zones of high to fluid overpressure?),
- exhibit unclear spatio-temporal associations with large seismic events (causal relation between modes of slip at different slip rate?)

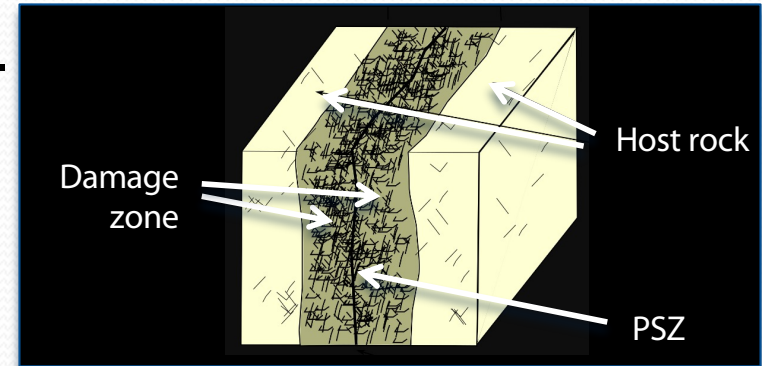


**Fault styles in onland exhumed structures**

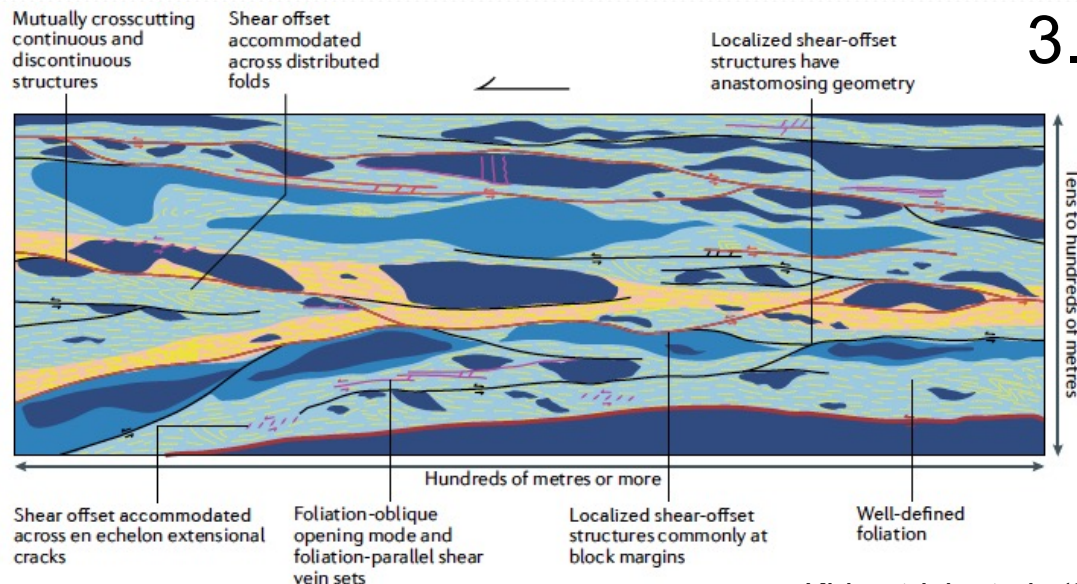
High-strain zones geometries/structures varies depending on rheology and degree of localization (e.g. Fagereng and Sibson, '10):

1. localized faults with a discrete, narrow principal slip zones (PSZs) surrounded by damage zones (Chester and Logan '86);
2. thick homogeneous layers of viscous material;
3. thick delocalized fault zones with mixture of heterogeneous materials and heterogeneous continuous-discontinuous deformation (Rowe et al., '13, Kirkpatrick et al, '21),

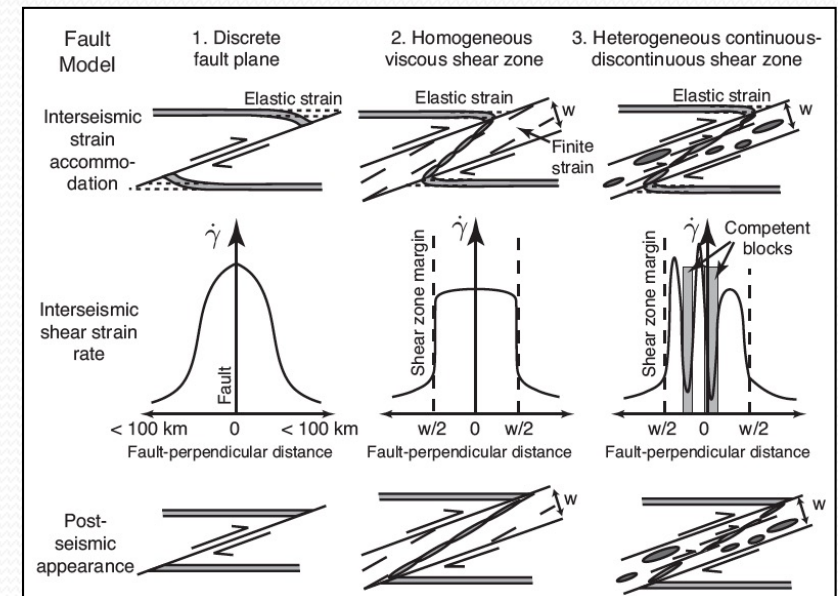
1.



3.



Kirkpatrick et al., '21



Fagereng and Sibson, '10

## FAULT STYLE VS. SLIP BEHAVIOR

1. Discrete, localized faults store elastic strain and episodically accommodate irrecoverable strain by seismic failure.
2. Homogeneous viscous shear zone accommodate most displacement by continuous, aseismic deformation (“stable sliding”);
3. Delocalized fault zones with heterogeneous distribution of deformation and materials with spatial variations in rheology (shear strength, viscosity, shear strain rate) and faulting style: elastic strain is released heterogeneously in slip surfaces within the shear zone (“unstable sliding”).

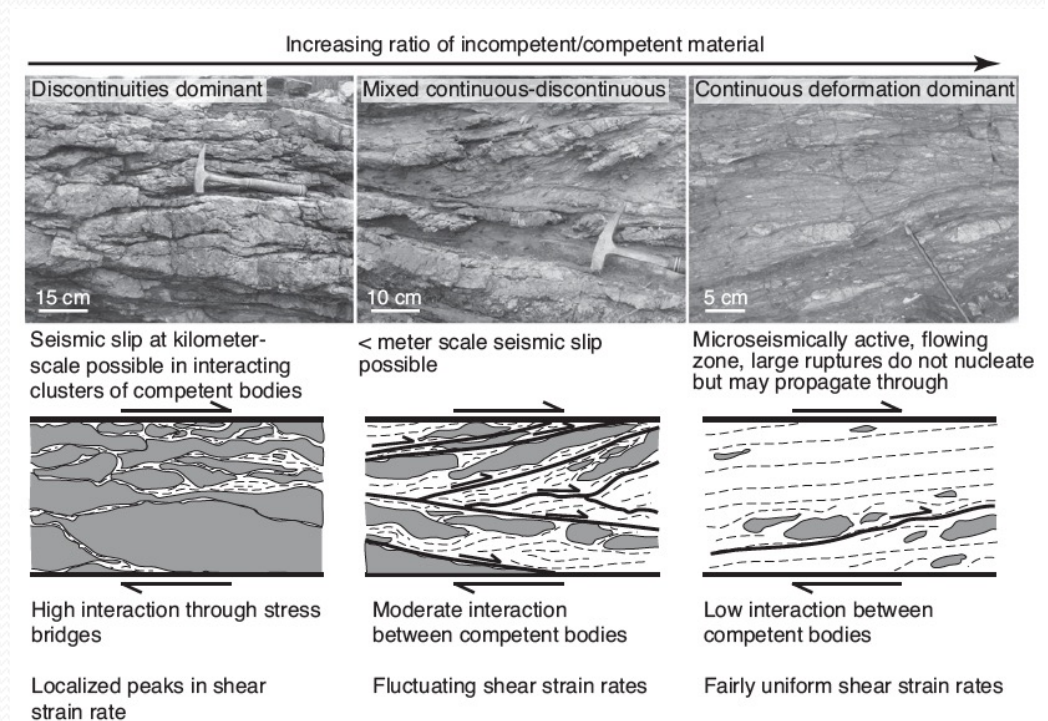
### IN THE SPACE BETWEEN

A wide range of fault rocks and textures are recorded on land as falling between 1. and 2. :

- this variety is time-dependent, and may represent a progression in fault evolution;
- the “seismic character” of this variety can be modeled in terms of incompetent vs. competent ratio

*(e.g. SSEs are widely thought to be a manifestation of transitional frictional stability)*

**Is the “space between” fault styles the record of “in between” slip behaviors?**

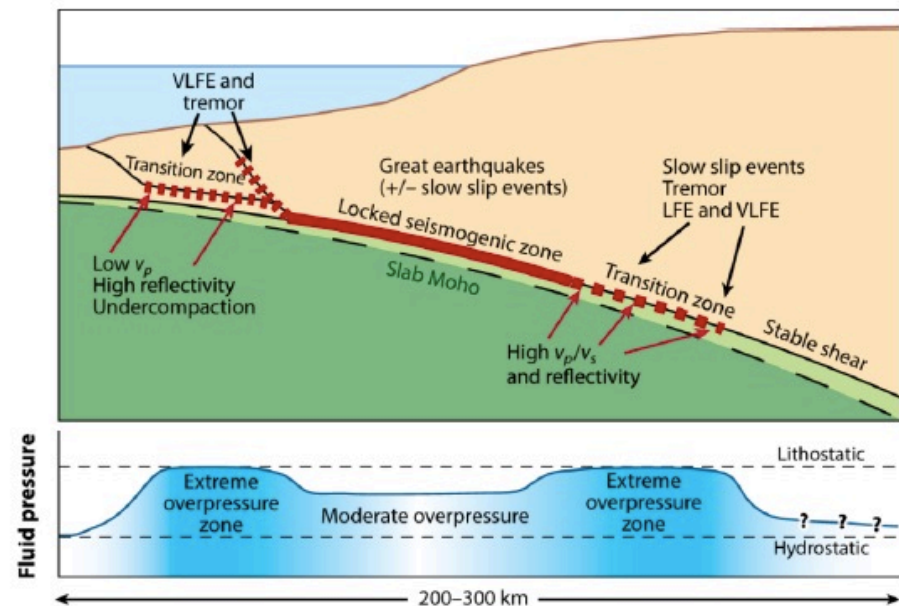


## SUBDUCTION ZONE SLIP STYLES: OPEN QUESTIONS

Steady creep, coseismic slip, and the variety of «slow earthquakes» in between (LFE, SSEs, tremors etc.), all contribute to plate motion accommodation along subduction thrust faults during the seismic cycle.

However:

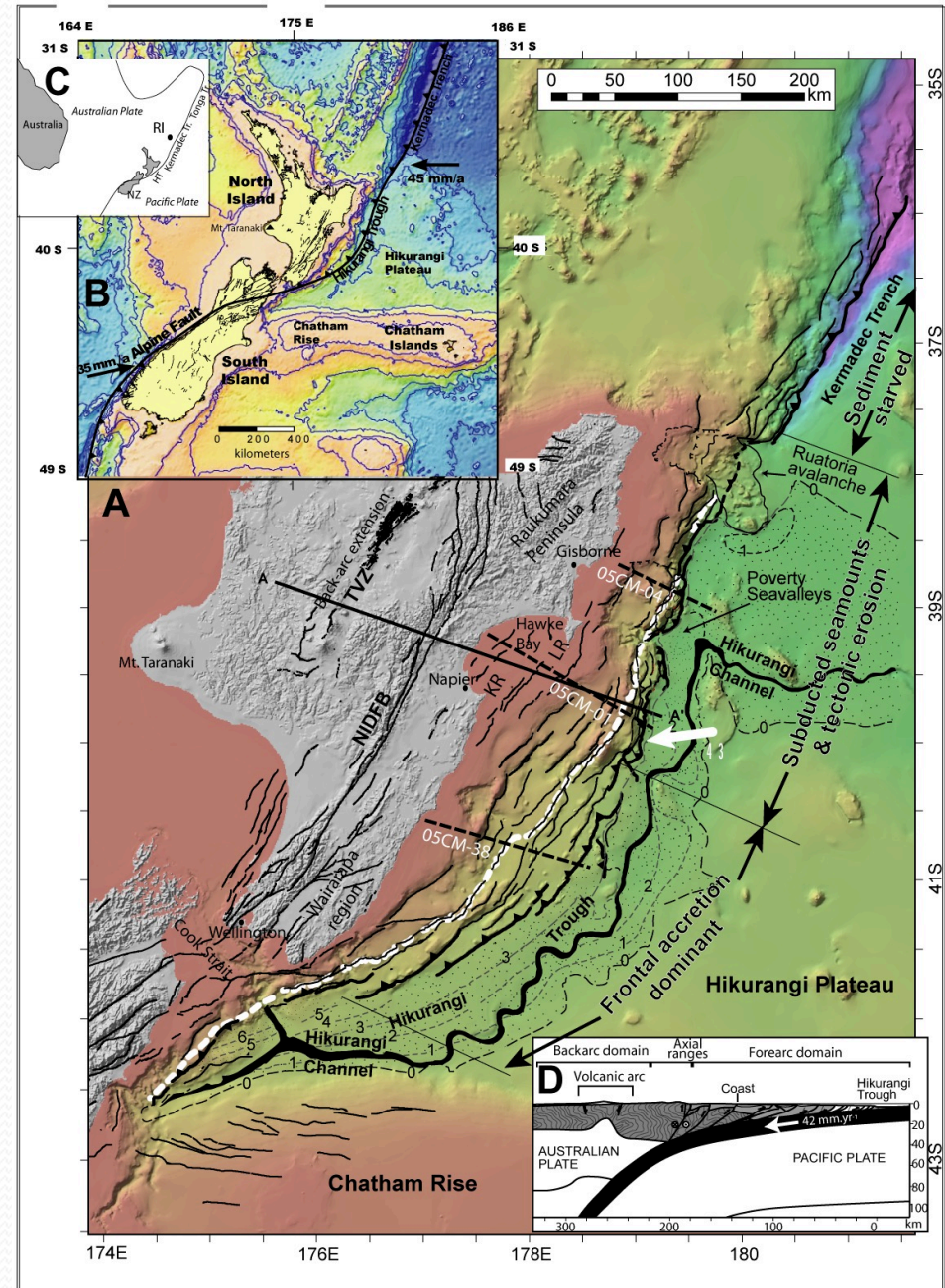
- we do not know exactly the underlying mechanisms promoting one fault behavior vs. another (i.e. the role of fluids in the transition from stable to unstable sliding);
- we do not know the relationships between “slow earthquakes” and destructive seismic slip (precursor? consequent?);
- we do not know unambiguously the deformation processes and geological signature of the different fault slip styles.



Existing hypotheses to explain “the space between” variety include: **contrasting material properties** entering the plate interface and promoting mixed behavior (Ando et al., '12; Skarbek et al., '12) and **low effective stress** (by high fluid pressures) promoting transitional frictional stability (Liu and Rice, '07; Segall et al., '10)

*The Hikurangi subduction margin*

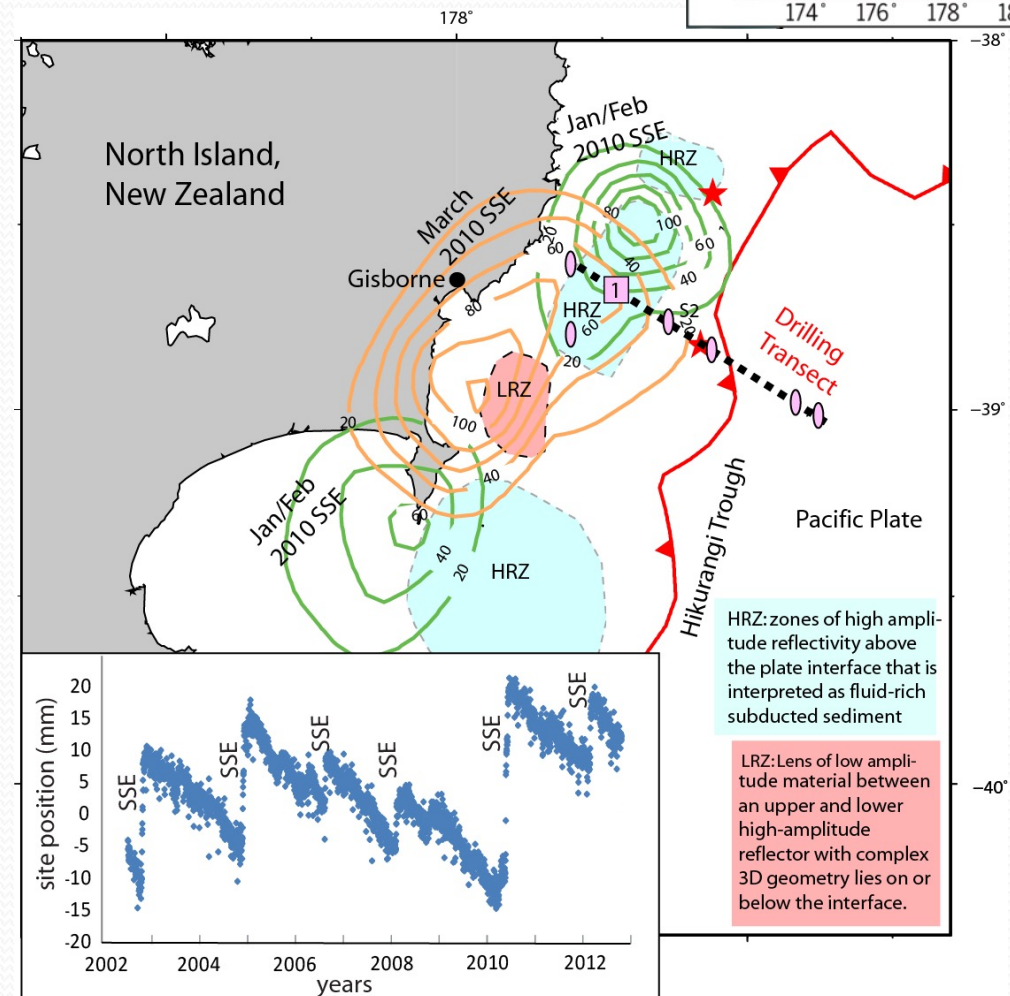
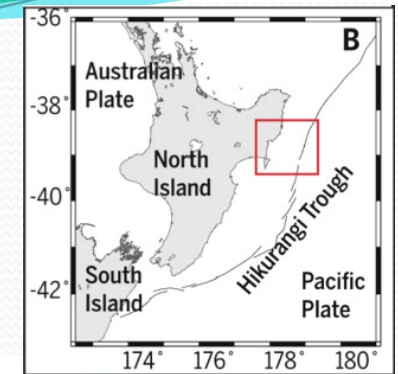
- Pacific plate is being subducted at the Hikurangi Trough at a rate of ~20 mm/yr beneath South Island and ~60 mm/yr beneath North Island
- Hikurangi Plateau is a Cretaceous large igneous province blanketed by ~1 to 1.5 km of sediment and studded with protruding basaltic seamounts
- Sedimentary cover is thicker at the Southern margin, due to sedimentation being funnelled along the Hikurangi channel from the South Island
- Southern Hikurangi margin has a well-developed accretionary wedge, while the Northern portion of the margin shows smaller prism and seamount subduction.



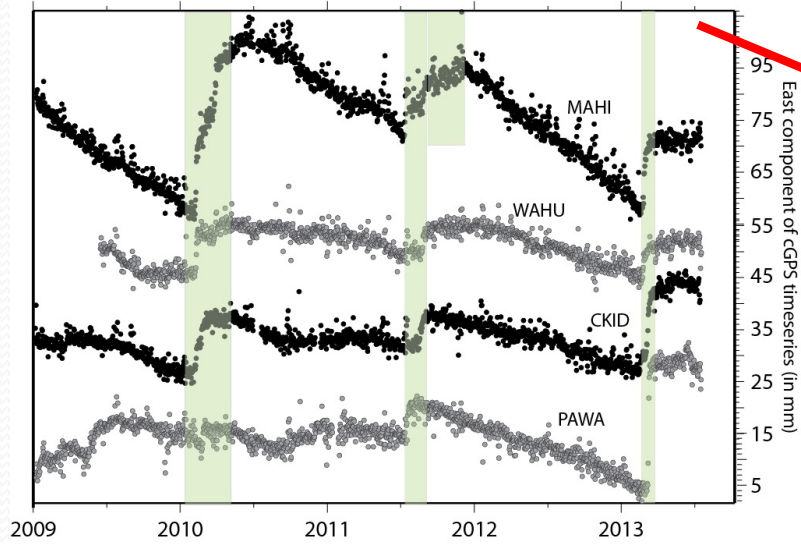
Hikurangi Margin hosts the shallowest geodetically well-documented SSEs on Earth :

The net of continuous GPS measurements indicates:

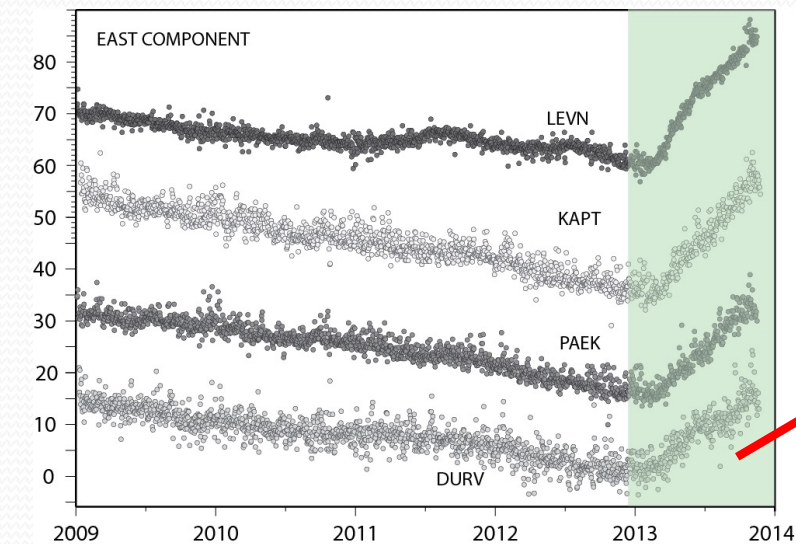
- ✧ SSEs last for days/weeks, recur **every 1-2 years**, show 1-3 cm of seaward surface displacement measured along the coastline (7-25 cm on the plate interface)
- ✧ Slow slip occurs **within 2 km to the trench**, potentially all the way to the trench: **material hosting SSEs can be reached by drilling.**



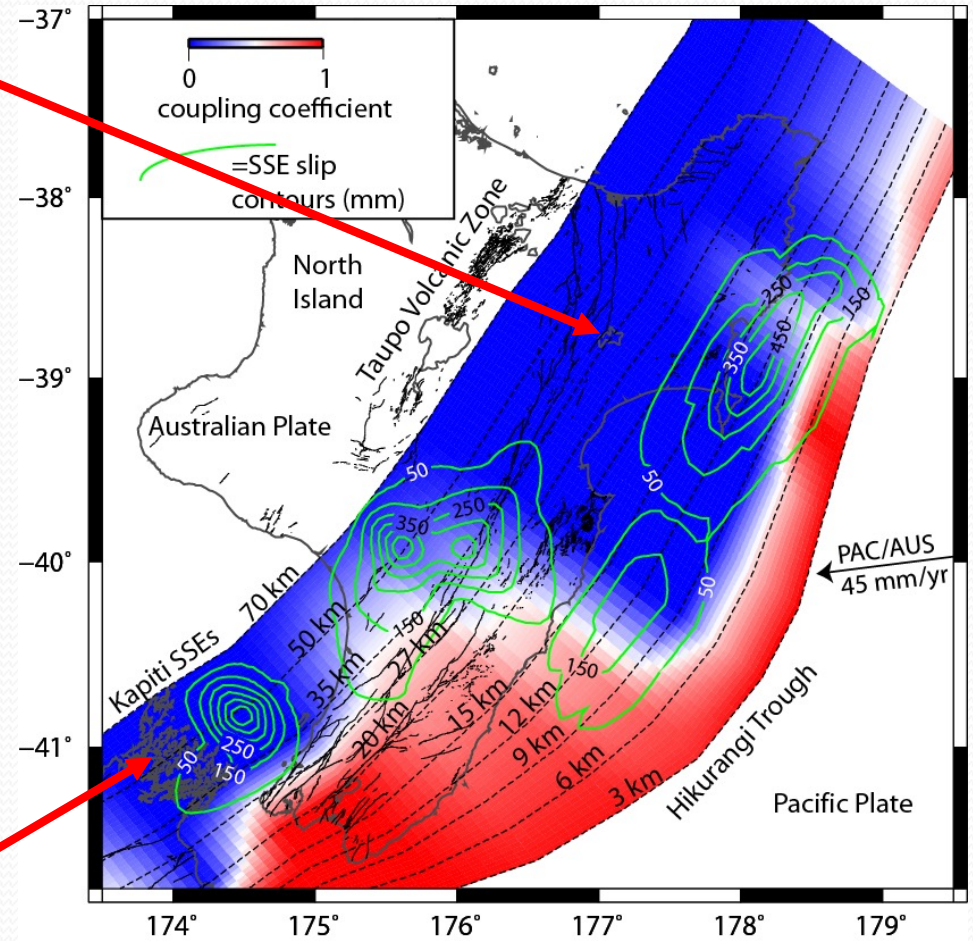
North Island vs. South Island SSEs



North  
Shallow,  
fast, large,  
frequent



South:  
Deep, slow,  
large, less  
frequent



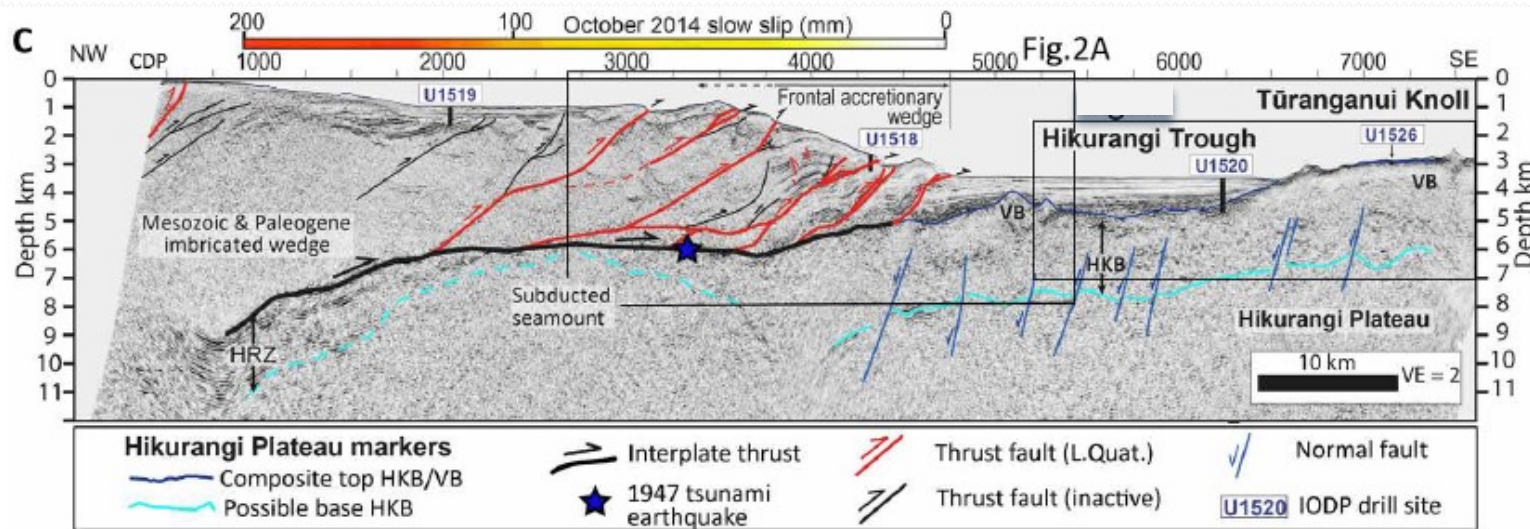
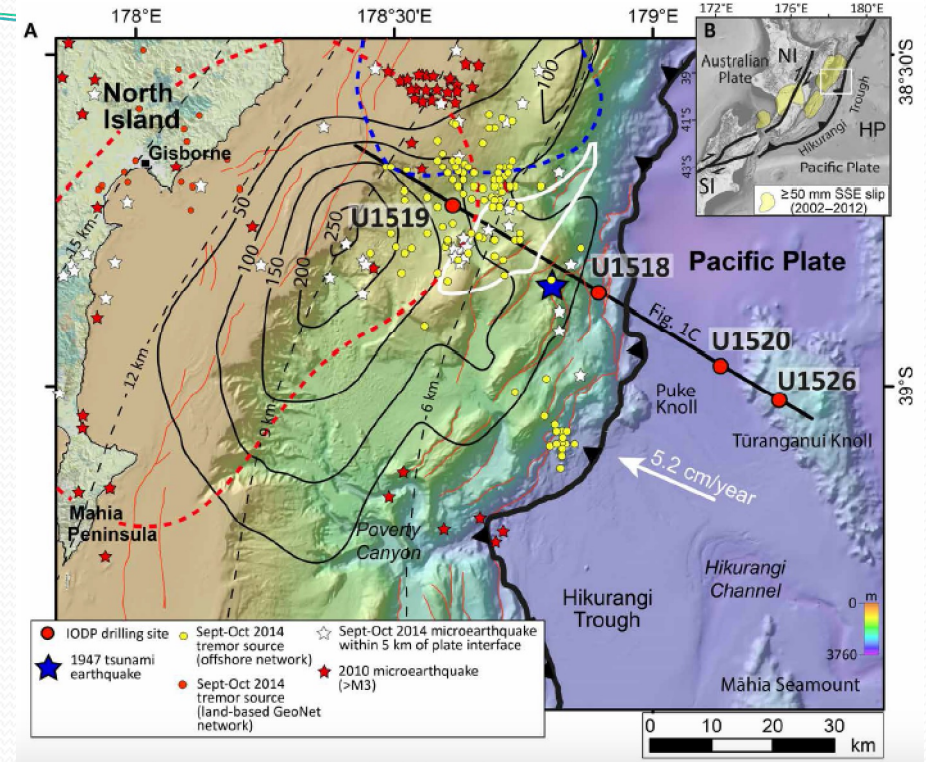
Green contours: cumulative slow slip 2002-2012  
Equivalent Mw 6.5-7.0 for deep & shallow SSEs

# Expedition 375 starts!

2 Expeditions Legs 372 (LWD) and 375 focused on the large, very shallow and frequent SSEs at the North Hikurangi Margin.

The plate interface hosted two Mw 7.0 to 7.2 earthquakes in 1947, which generated 8- to 10-m tsunami along the coast.

Exp 375 provided coring and sampling, and observatory installation, and comprised 58 days at sea, from 8 March to May 5 2018.



## Expedition 375 scientific targets

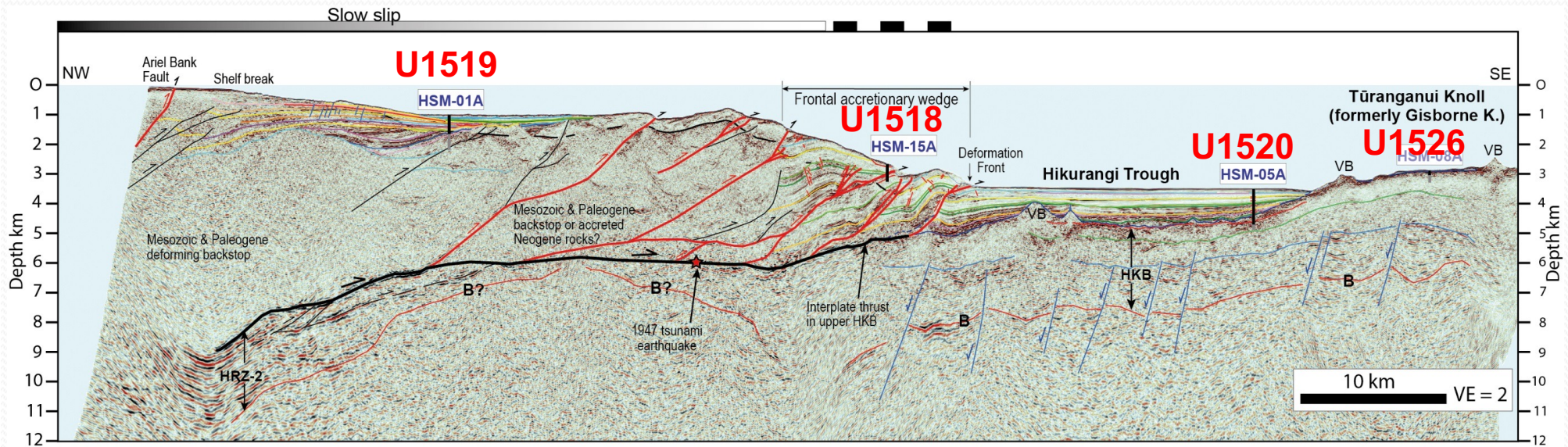
- 1) Characterize** the compositional, thermal, hydrogeological, frictional, geochemical, structural, and diagenetic conditions **the incoming plate and shallow plate boundary fault** near the trench (protolith and initial conditions for fault zone rock at greater depth, which may itself host shallow slow slip)
- 2) Characterize** material properties, thermal and stress conditions in **the upper plate** above SSEs source area, and
- 3) Monitoring** of deformation, temperature, fluid flow via borehole observatories at an active thrust near deformation front.

In this time together I will show you how we reconstructed the stratigraphy, composition, geometry, and physical properties of the lower plate entering the plate interface, by combining drilling results with regional seismic reflection profiles, in order to check working hypothesis 3:

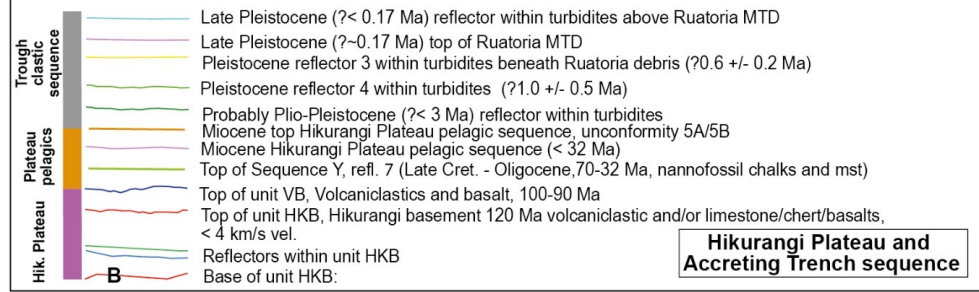
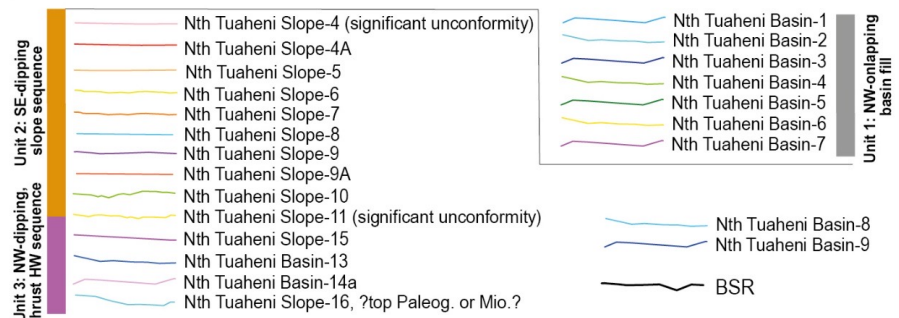
**3. SSEs occur in regions of conditional frictional stability (multiple slip behavior of a single fault patch), i.e. contrasting material properties entering the plate interface may promote mixed slip behavior.**

Then I will show how we experimentally tested the ability of the rocks and sediments along the drilled shallow thrust of propagating an earthquake rupture, a societal problem of primary interest given the risk for seismic slip at shallow crustal depths to generate tsunamis

# Four Primary sites across seismic profile 05CM-04



## Upper margin - north Tuaheni Basin



Lower margin and Hikurangi Trough seismic stratigraphy modified from Davy et al., 2008; Barnes et al., 2010; Plaza-Faverola et al., 2012; Ghisetti et al., 2016; Barnes et al., accepted

Seismic depth section processed by Dan Barker (GNS Science, NZ): 05CM-04 PSTM HDVA-8 model

\*Note revised interpretation cf. Science Prospectus 2017

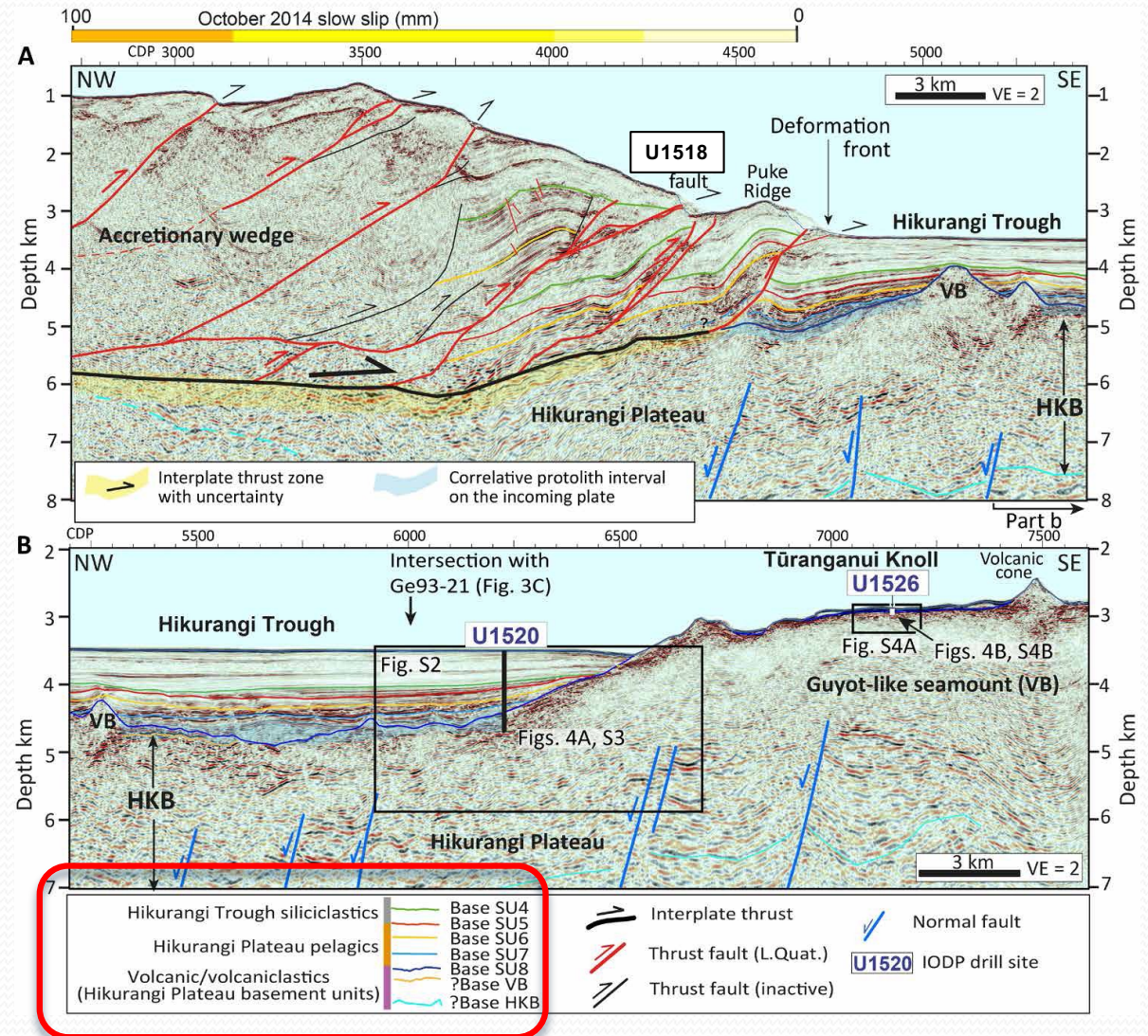
# The Primary sites across the incoming plate: U1520 and 1526

## What geophysics tells us

Seismic profiles show a typical frontal side of the accretionary prism, with shallow thrusts branching off a basal plate interface.

The zoom on the lower plate show a rough topography (top of HKB and VB) with imminent arrival of a seamount into the system.

*Seismic units (SU) vs. borehole data correlation*



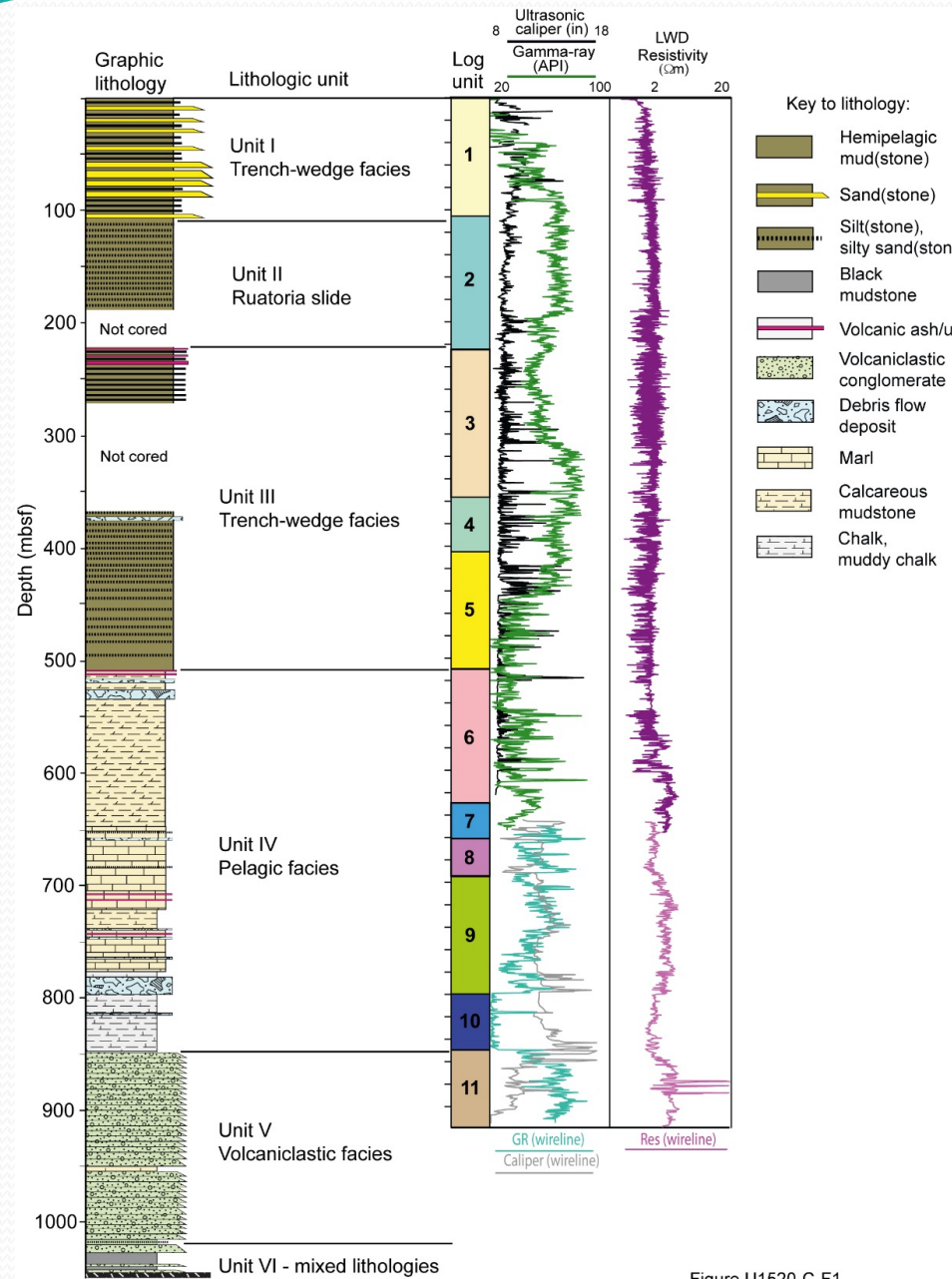
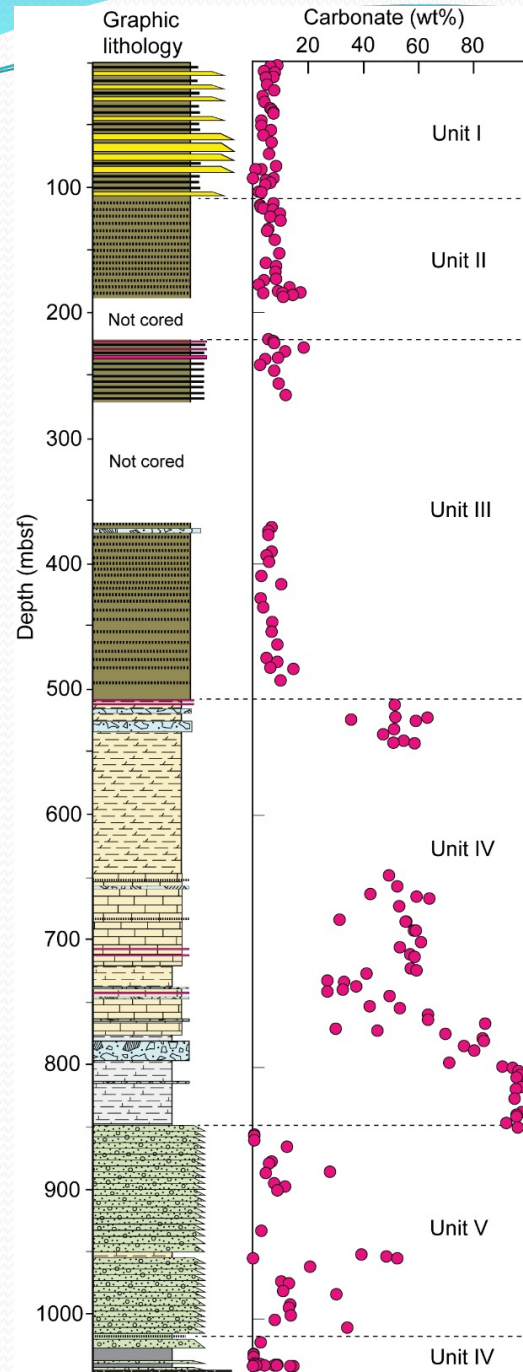


Figure U1520-C-F1

## Input site: stratigraphy of Site U1520 reconstructed from Hole D and C

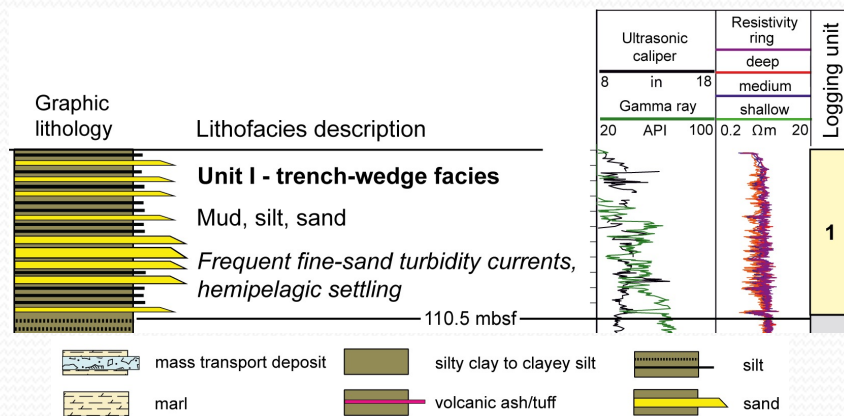
- 6 Units defined on the base of texture, sedimentary structures, thickness of coarse bed, soft-sediment def., carbonate content etc.
- Change from terrigenous-clastic gravity-flow deposits, to a pelagic carbonate sedimentation, down to volcaniclastic gravity-flow system
- Early Cretaceous to Holocene



## Carbonate content vs. depth

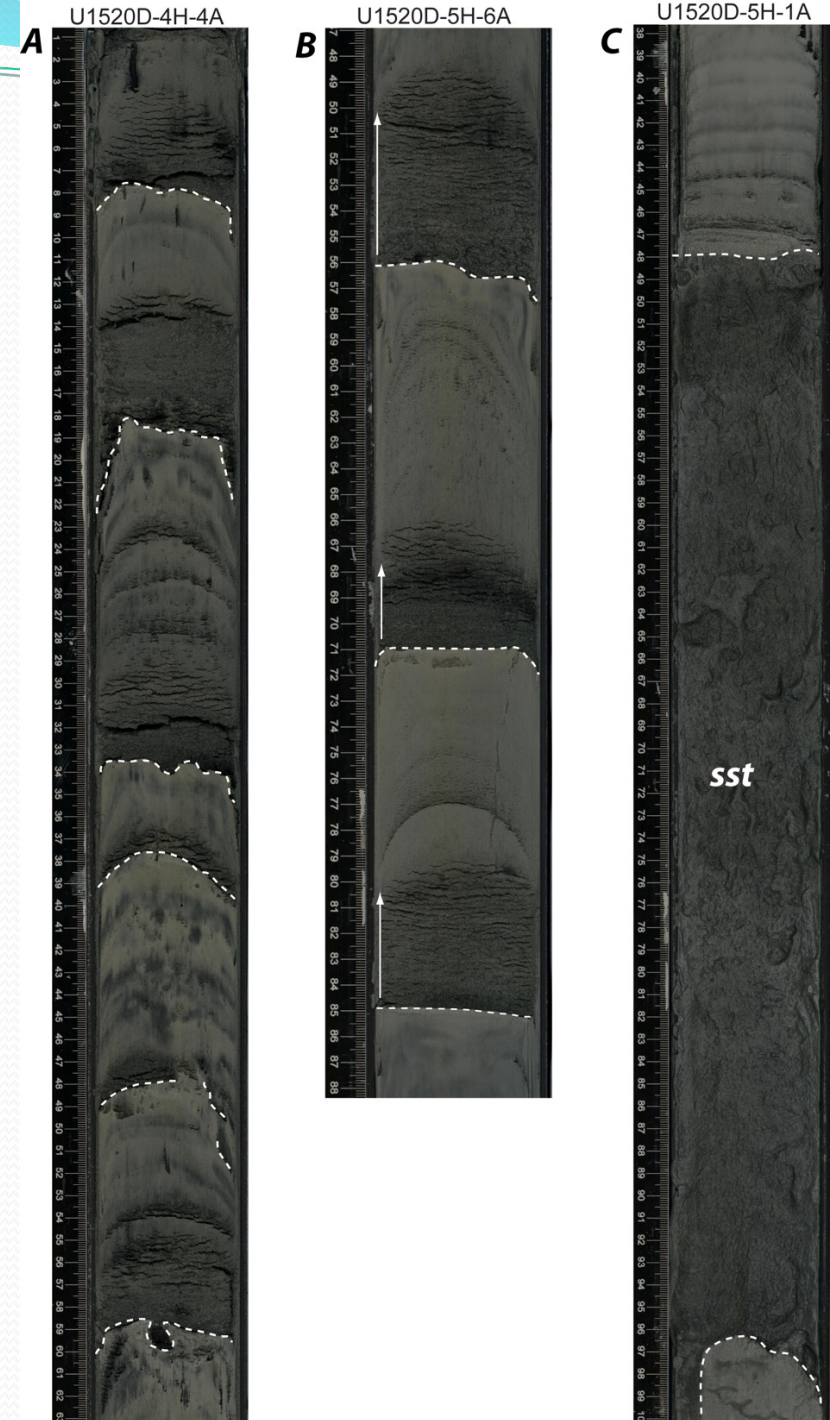
- Change from terrigenous-clastic gravity-flow deposits, to a pelagic carbonate sedimentation, down to volcanoclastic gravity-flow system

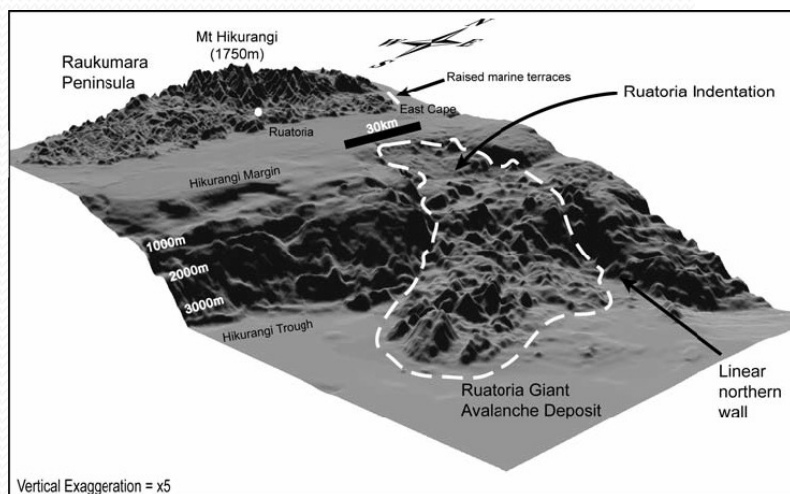
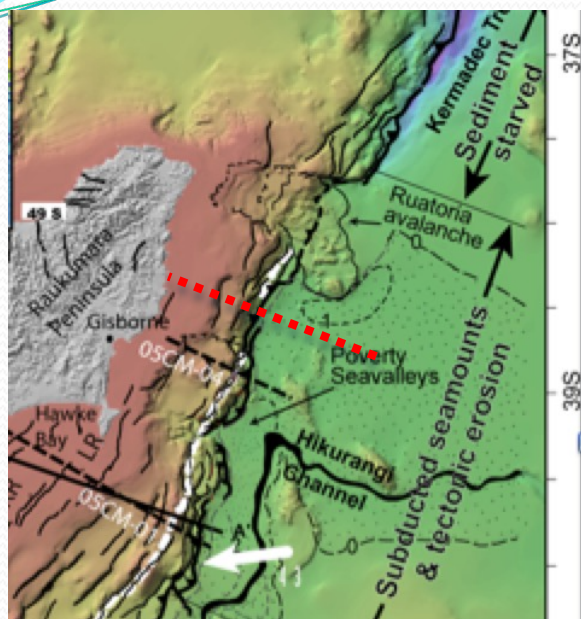
# Unit I: trench-wedge



Thin- to medium-bedded turbidites, sharp bases, normal grading.

**Holocene - Pleistocene**

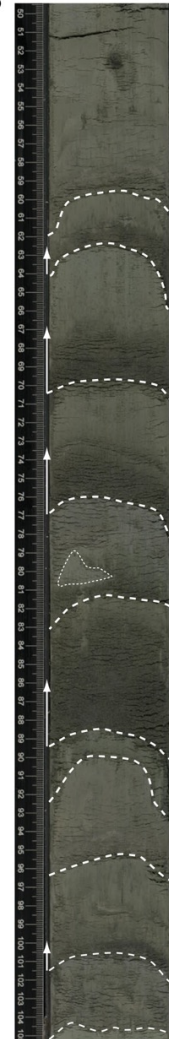




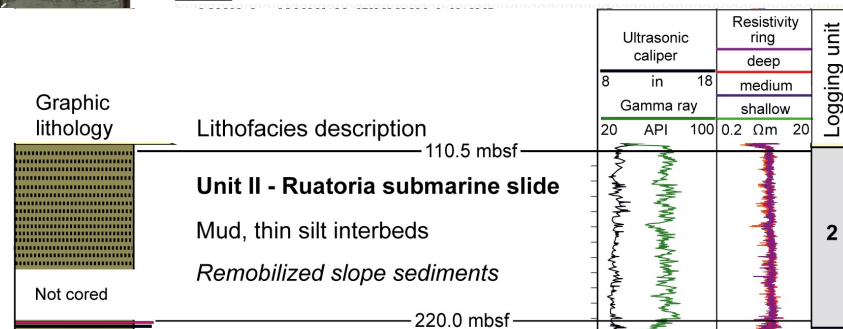
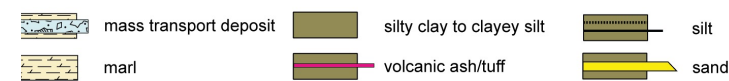
A U1520D-13H-2A

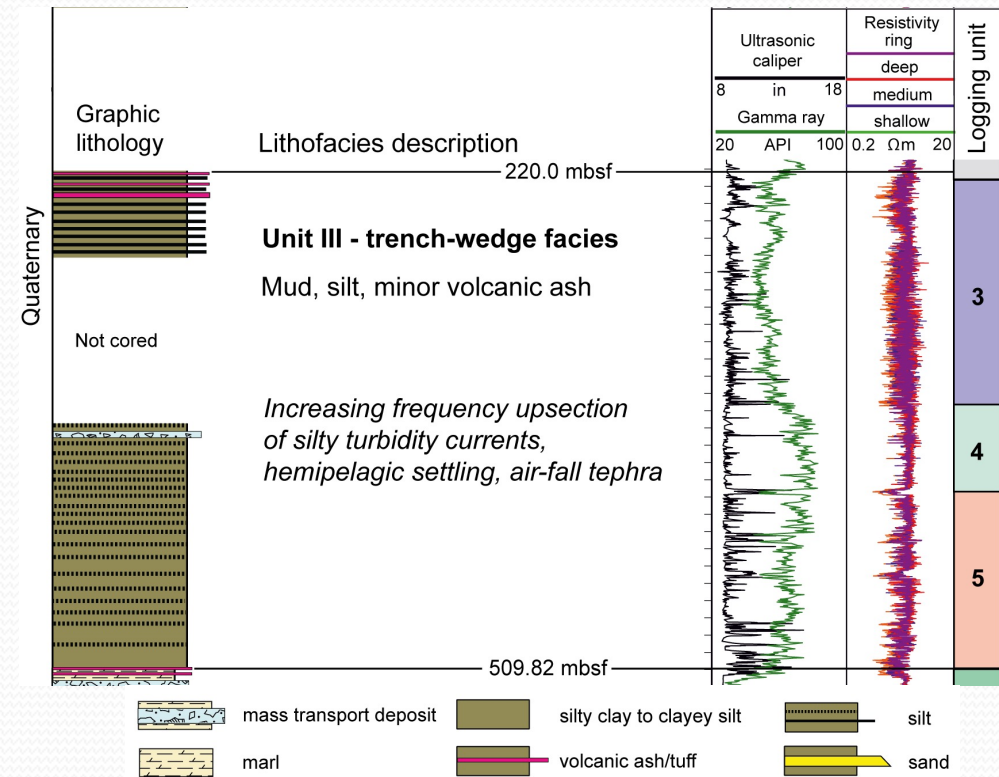


B U1520D-30F-2A



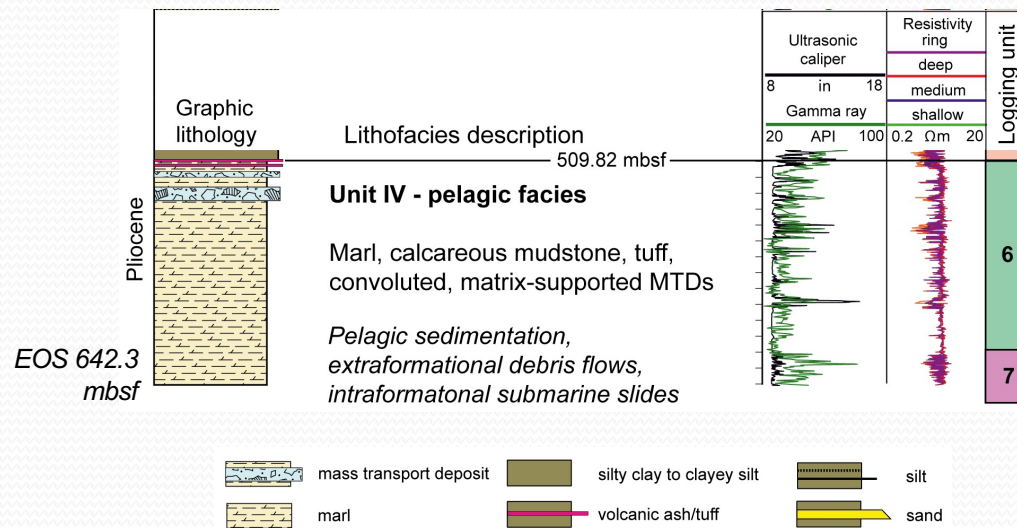
- thin-bedded silty turbidites with nearly equal intervals
- reduction of thickness and frequency of coarse interbeds compared to Unit I
- mud intraclasts and erosional basal contacts
- NO EVIDENCE of gravity-driven remobilization/deformation





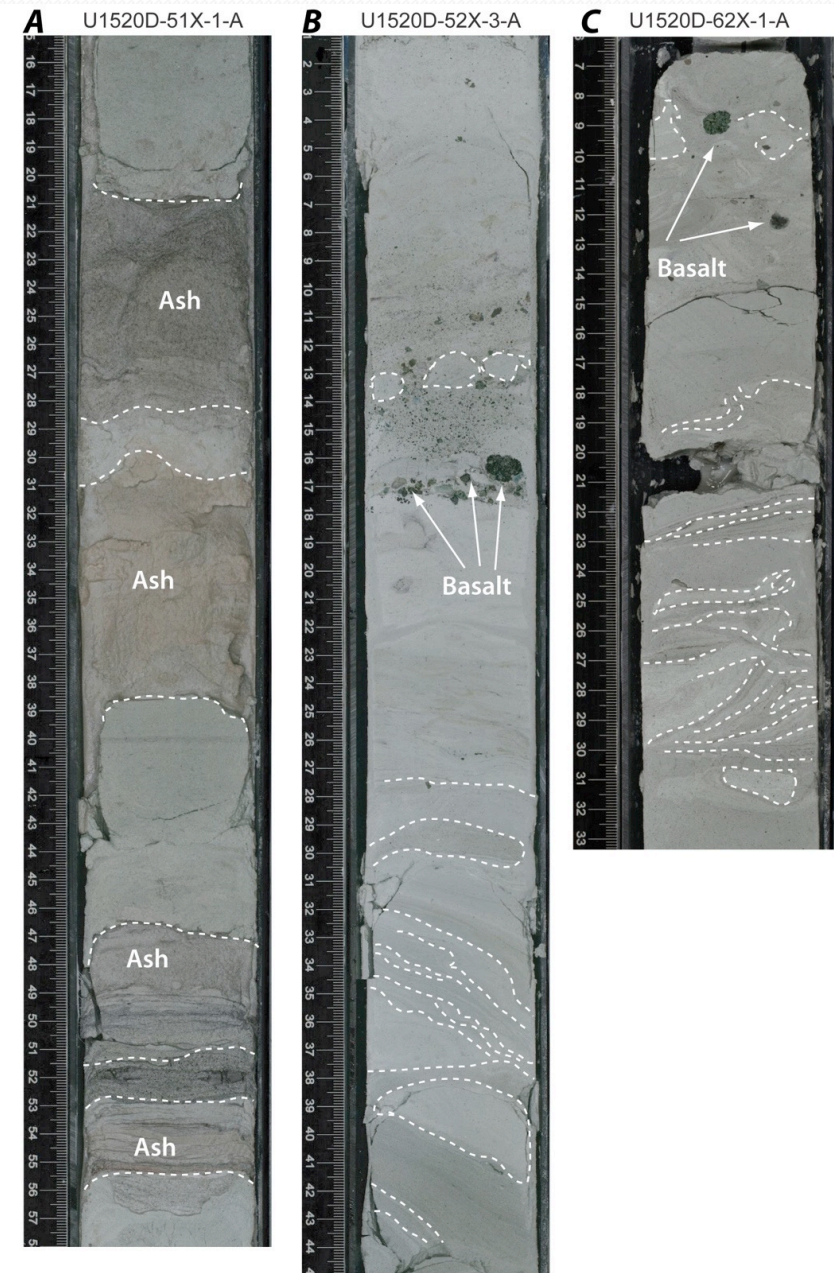
- normally-graded thin-bedded turbidites with planar laminations
- medium- to thick-bedded ash layers
- mass transport deposits (MTDs), convoluted layers, mud “clasts”

# Unit IV: Hole D

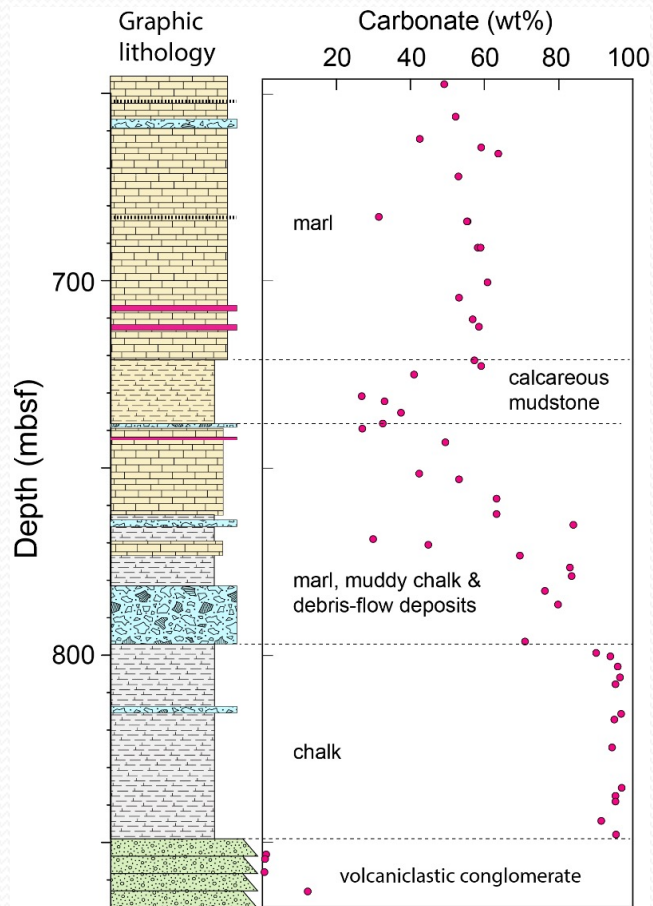


- Light greenish-gray strongly bioturbated marls
- Convoluted marl layers, flow banding structures, block-in-matrix textures, sand- to pebble-size basalt and marl clasts,
- Ash layers

**Paleocene to Miocene**



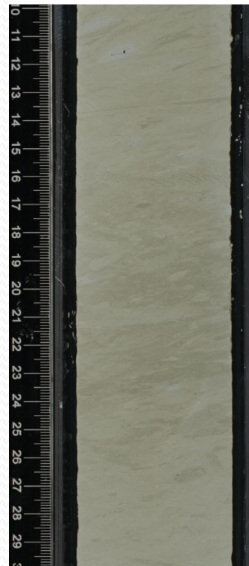
# Unit IV: Hole C



Unit IV was recovered in deeper hole as comprising marls, calcareous mudstone, chalk, and interbedded debris-flow deposits.

## Paleocene to Miocene

375-U1520C-10R-2A,  
10-30 cm



marl

(646-721.31 mbsf)

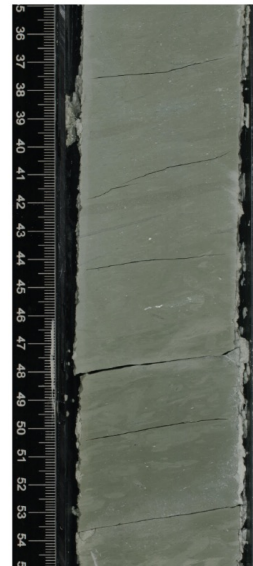
375-U1520C-10R-3A,  
10-30 cm



calcareous  
mudstone

(721.31-738.68 mbsf)

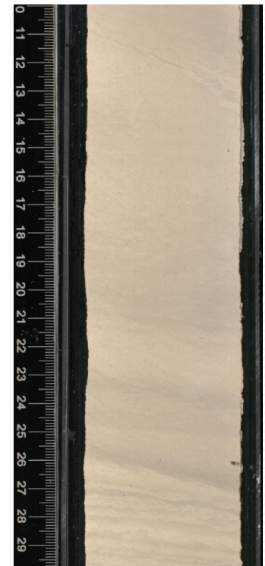
375-U1520C-15R-3A,  
35-55 cm



marl

(738.68-773.26 mbsf)

375-U1520C-16R-3A,  
10-30 cm

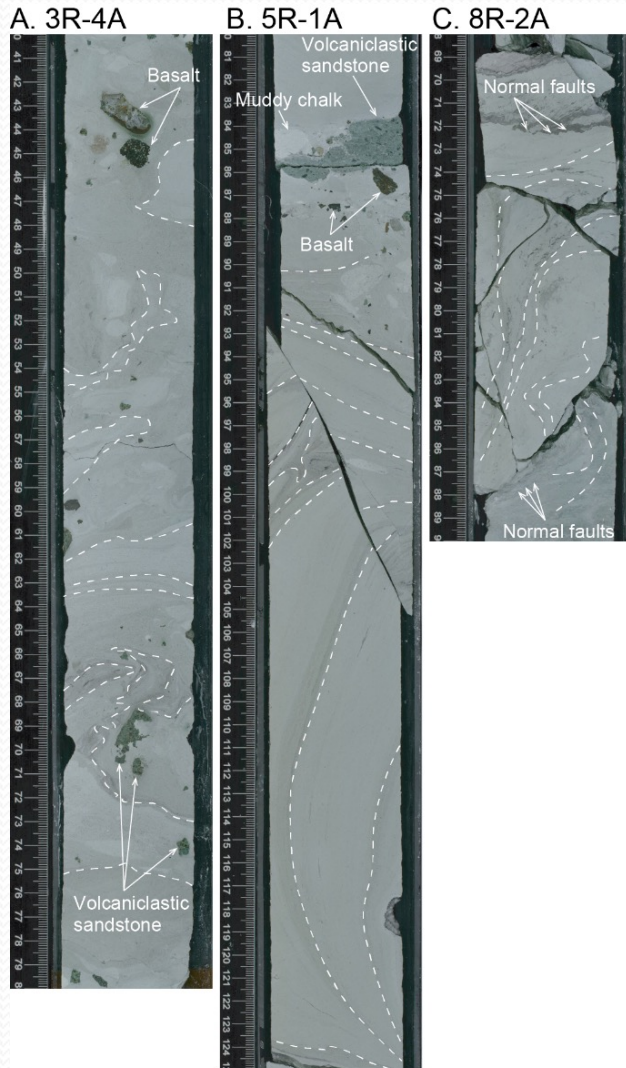


chalk

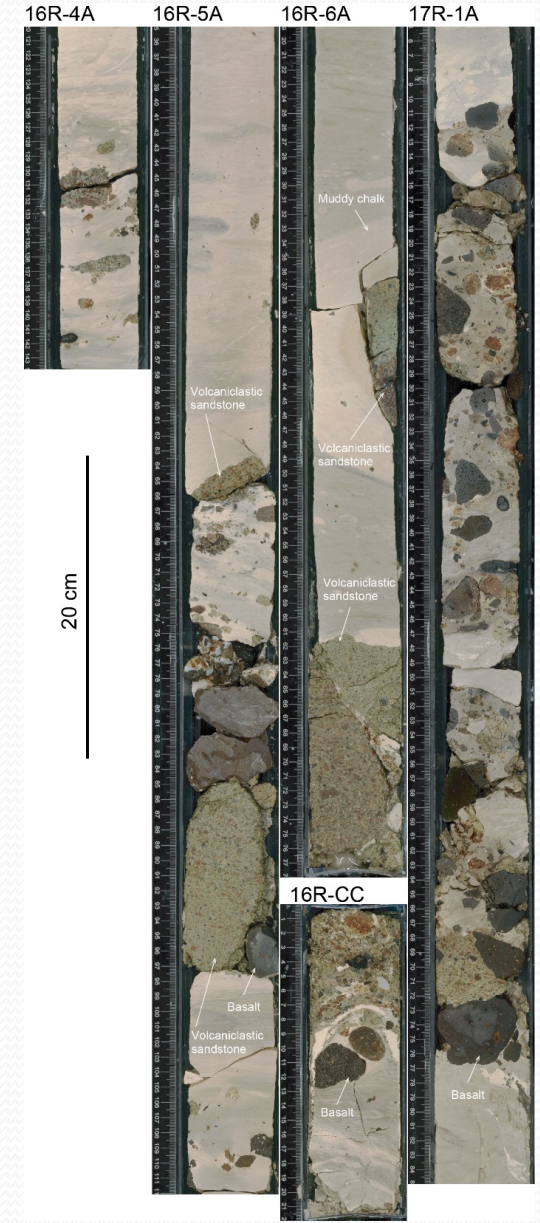
(773.26-848.45 mbsf)

Debris flows:  
 flow banding structures, block-in-matrix textures, sand- to pebble-size basalt and marl clasts

Convoluted marl beds



Debris flows



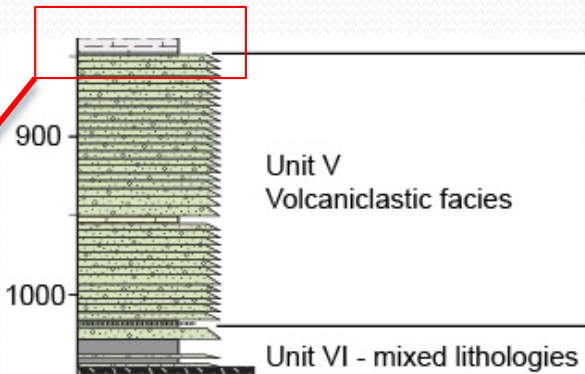
# Unit V

U1520C-23R-5-A, 30-59



Unit IV: slow pelagic settling  
vs.  
Unit V: high-density gravity flow

- Volcaniclastic granule-size Conglomerate
  - +  
• Marl (+Clayey siltstone, +Basalt)
- Upper Cretaceous**



U1520C-24R-2-A



U1520C-26R-1-A



U1520C-27R-6-A



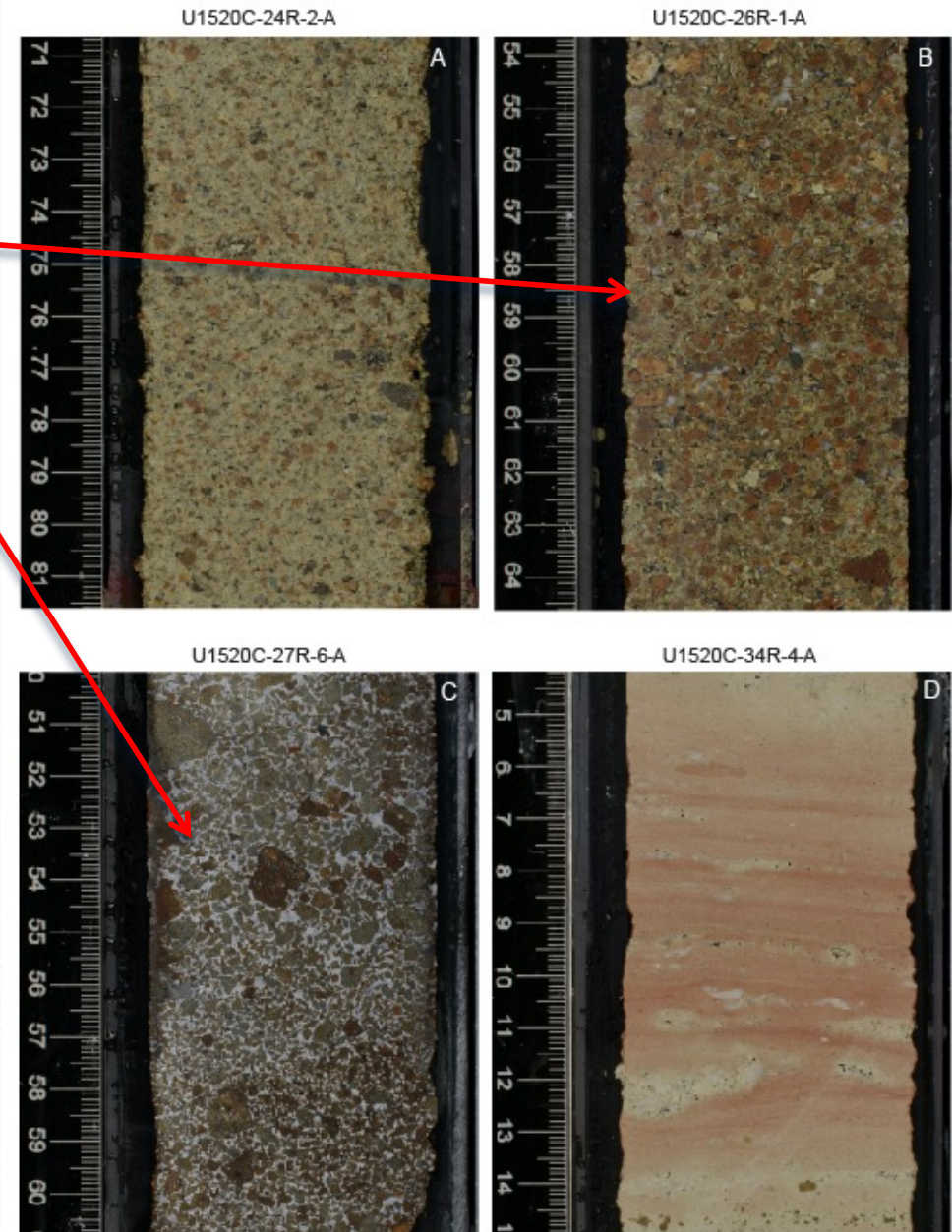
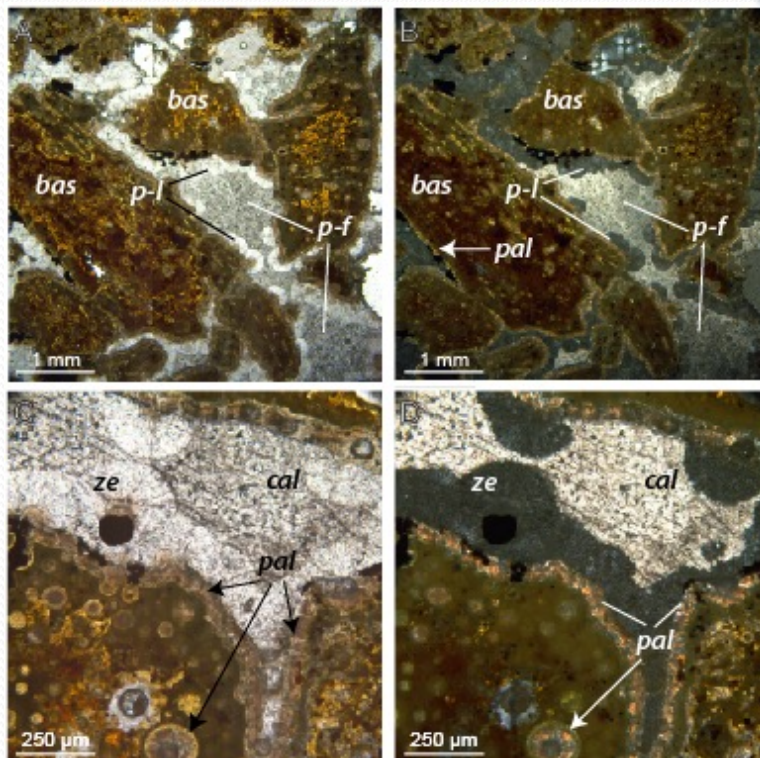
U1520C-34R-4-A



*Grain flow and debris flow mechanisms from the Tūranganui Knoll*

## Unit V

- Volcaniclastic granule-size conglomerate: clast-supported, clasts are tightly packed bound by pore-filling palagonite, zeolite and calcite cement (strong lithification)



*Grain flow and debris flow mechanisms from the Tūranganui Knoll*

## Unit VI

- drilled for > 200 m until basalts
- highly mixed assemblage of volcanoclastic conglomerate, volcanoclastic siltstone, silty claystone with minor limestone and organic-rich siltstone, and basalt with, unresolvable stratigraphic organization or thicknesses (poor recovery, coring disturbance, and “biscuiting”),
- distinctive dark blueish-green color is widespread among most of the rock fragments,
- siltstone with pyrite and high values of total organic carbon

### Upper Cretaceous

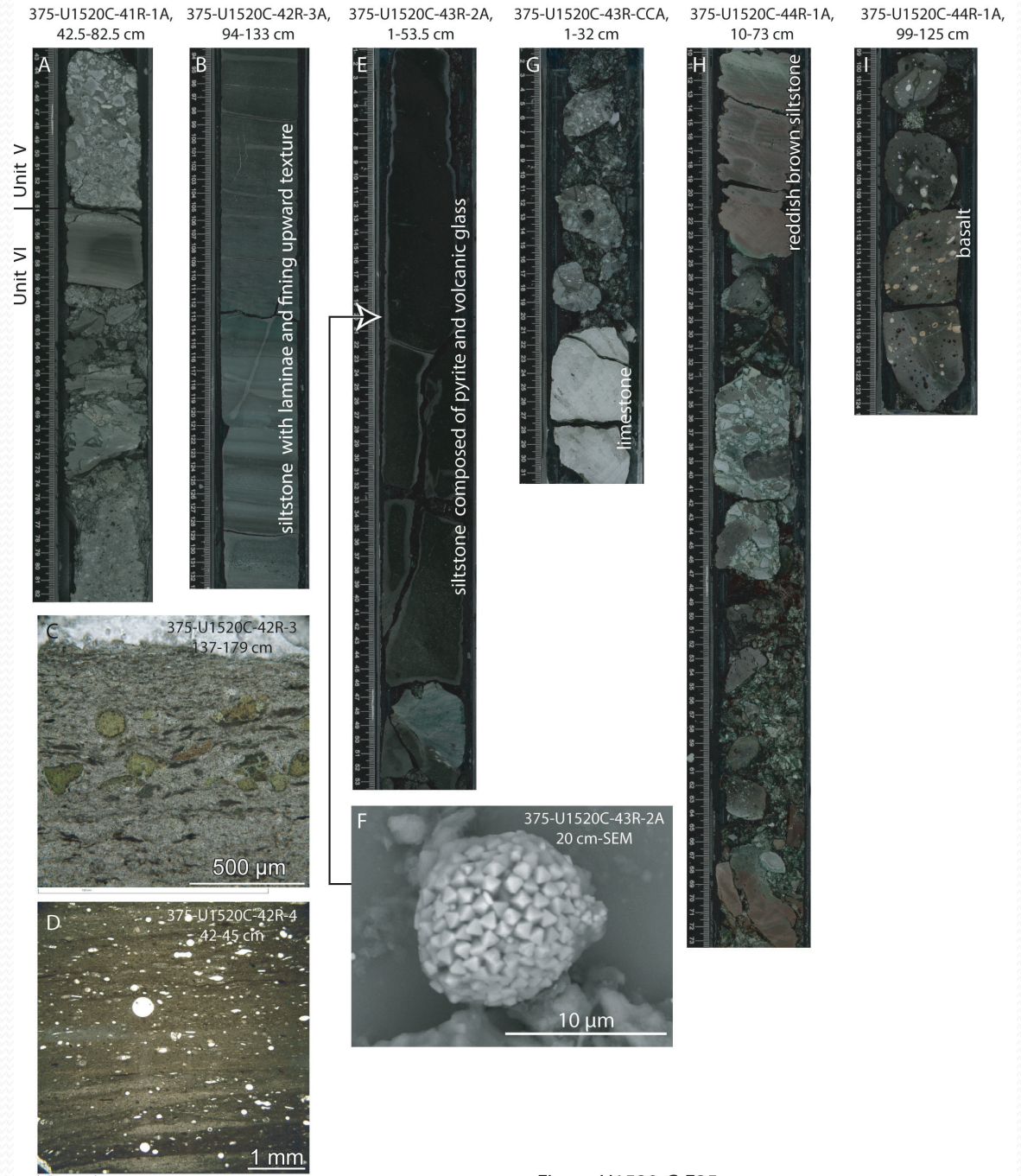
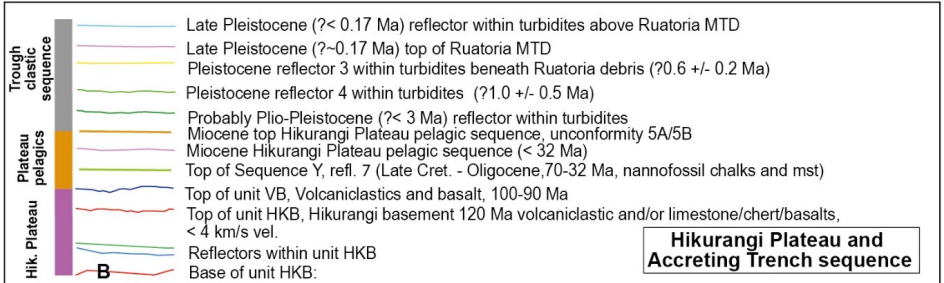
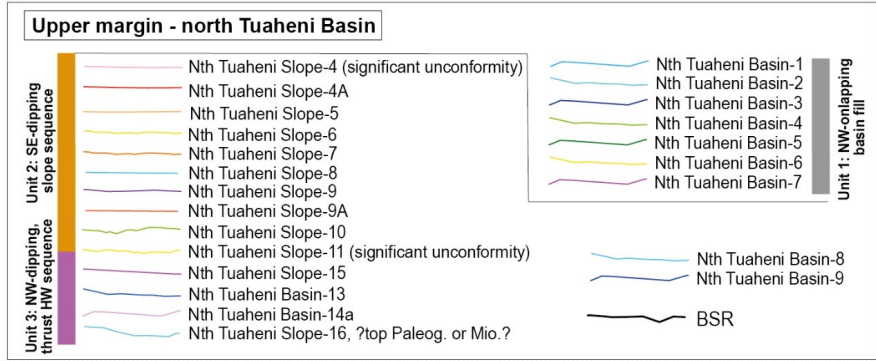
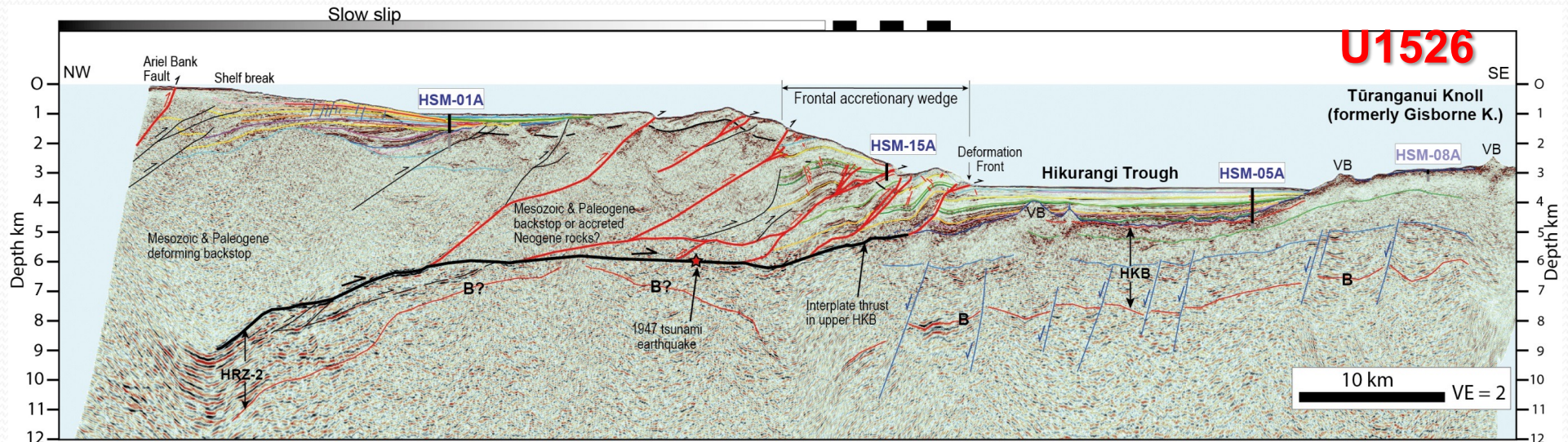


Figure U1520-C-525

# U1526: subducting seamount (Tūranganui Knoll)



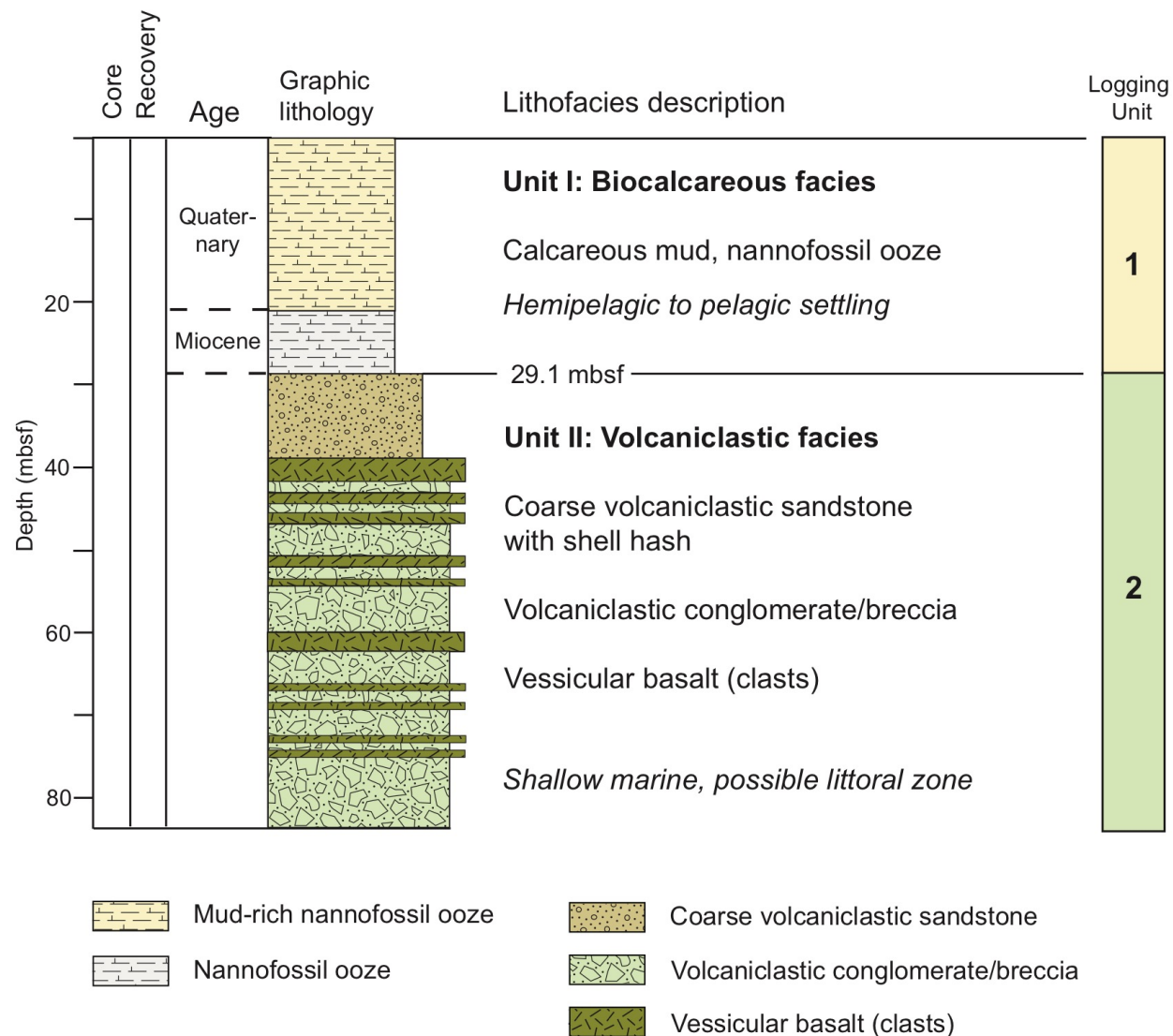
Lower margin and Hikurangi Trough seismic stratigraphy modified from Davy et al., 2008, Barnes et al., 2010, Plaza-Faverola et al., 2012, Ghisetti et al., 2016; Barnes et al., accepted

Seismic depth section processed by Dan Barker (GNS Science, NZ): 05CM-04 PSTM HDVA-8 model

Interpretation: Phil Barnes

\*Note revised interpretation cf. Science Prospectus 2017

# Stratigraphy of Site U1526: the Tūranganui Knoll



## Unit I: Biocalcareous facies

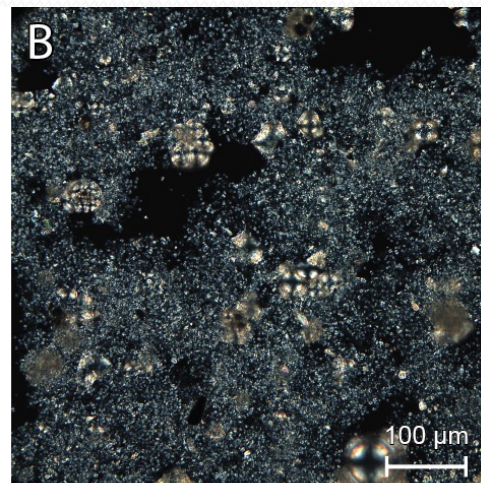
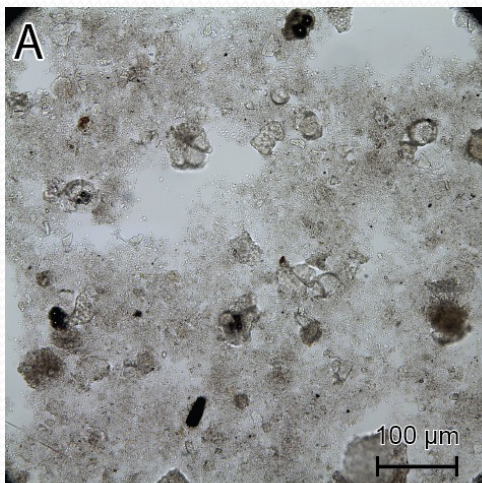
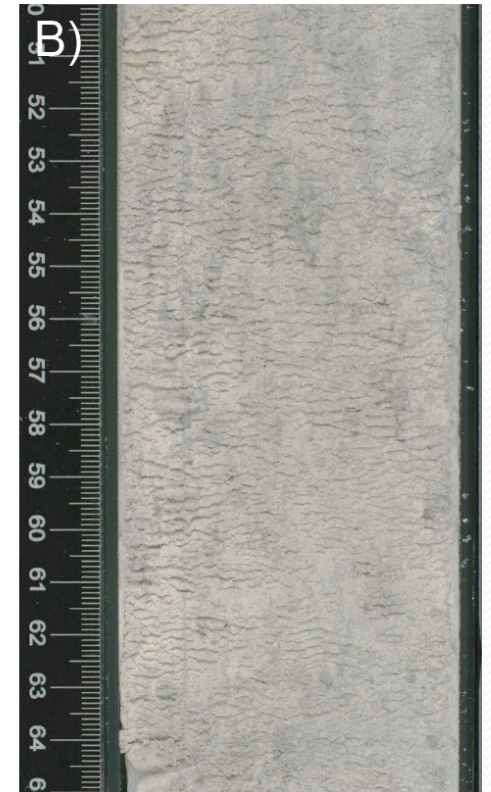
Calcareous mudstone  
and nannofossil ooze

(Late Cretaceous to Holocene)

U1526A-3R-1A, 5–20 cm



U1526A-3R-2A, 50–65 cm



## Volcaniclastic coarse sandstone and conglomerate

- A) Sandstone w/ basalt, bivalve shells, other calcareous bioclasts, limestone - planar laminated
- B) Sandstone to granule-size conglomerate w/ basalt and bivalve shell fragments shells are partly dissolved
- C) Pebble-cobble-boulder conglomerate rounded basalt and shell fragments – sandy matrix

U1526A-4R-1A, 5–30 cm

U1526A-4R-1A, 34–59 cm

U1526A-7R-2A, 8–33 cm



Calcite cementation.  
Pervasive reddish stain  
and bivalve suggest very  
shallow water and  
temporary subaerial  
exposure of seamount

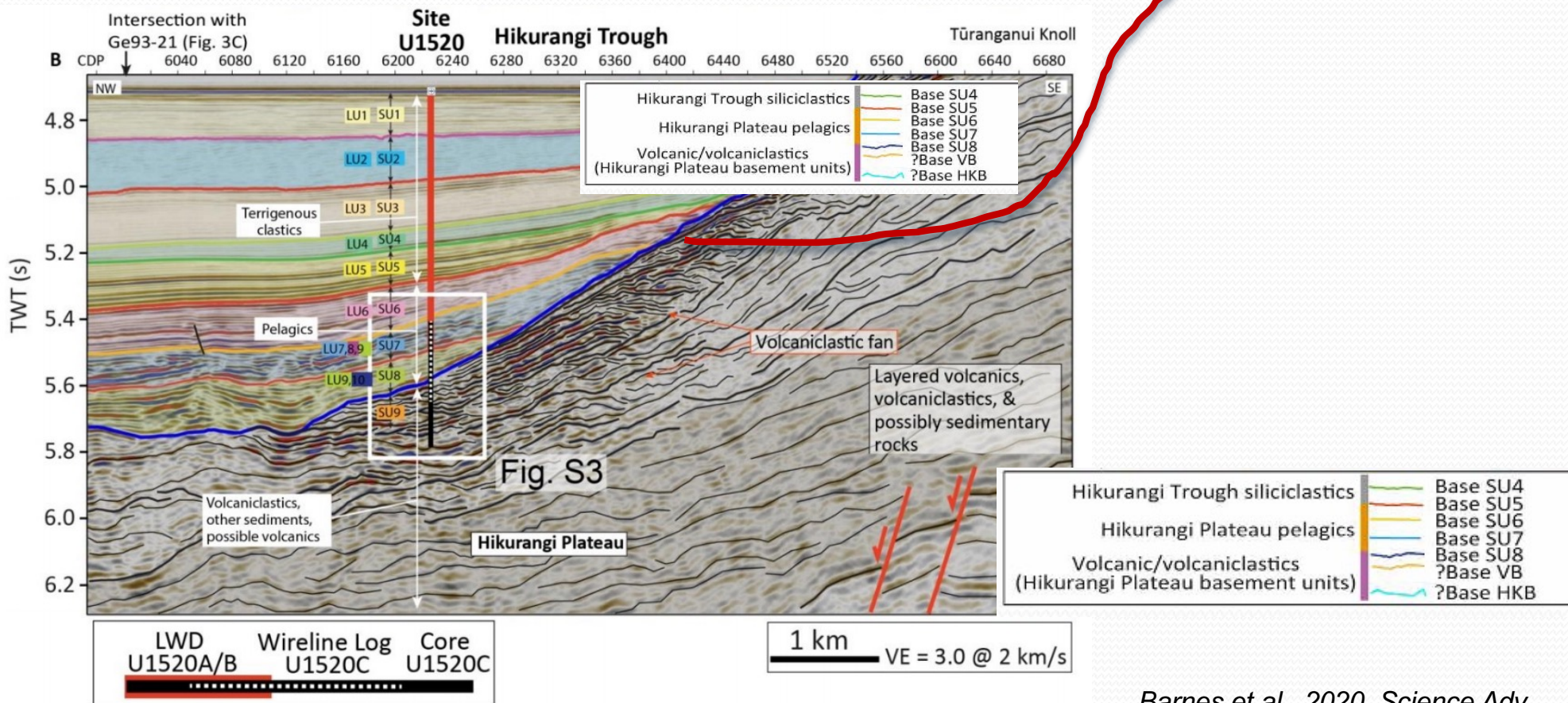
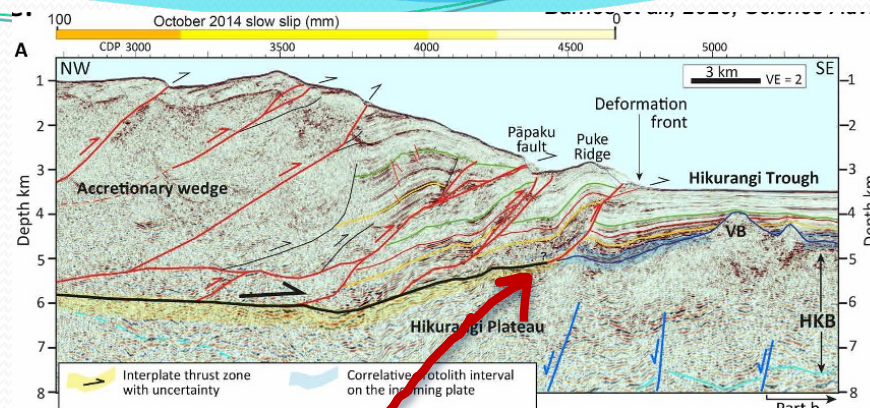
Boulder-size clast of fresh  
vessicular basalt clay)



# Core-log-seismic integration: a “geologic section” of the incoming plate

Core and logging data (LU) tied to seismic profile (SU).

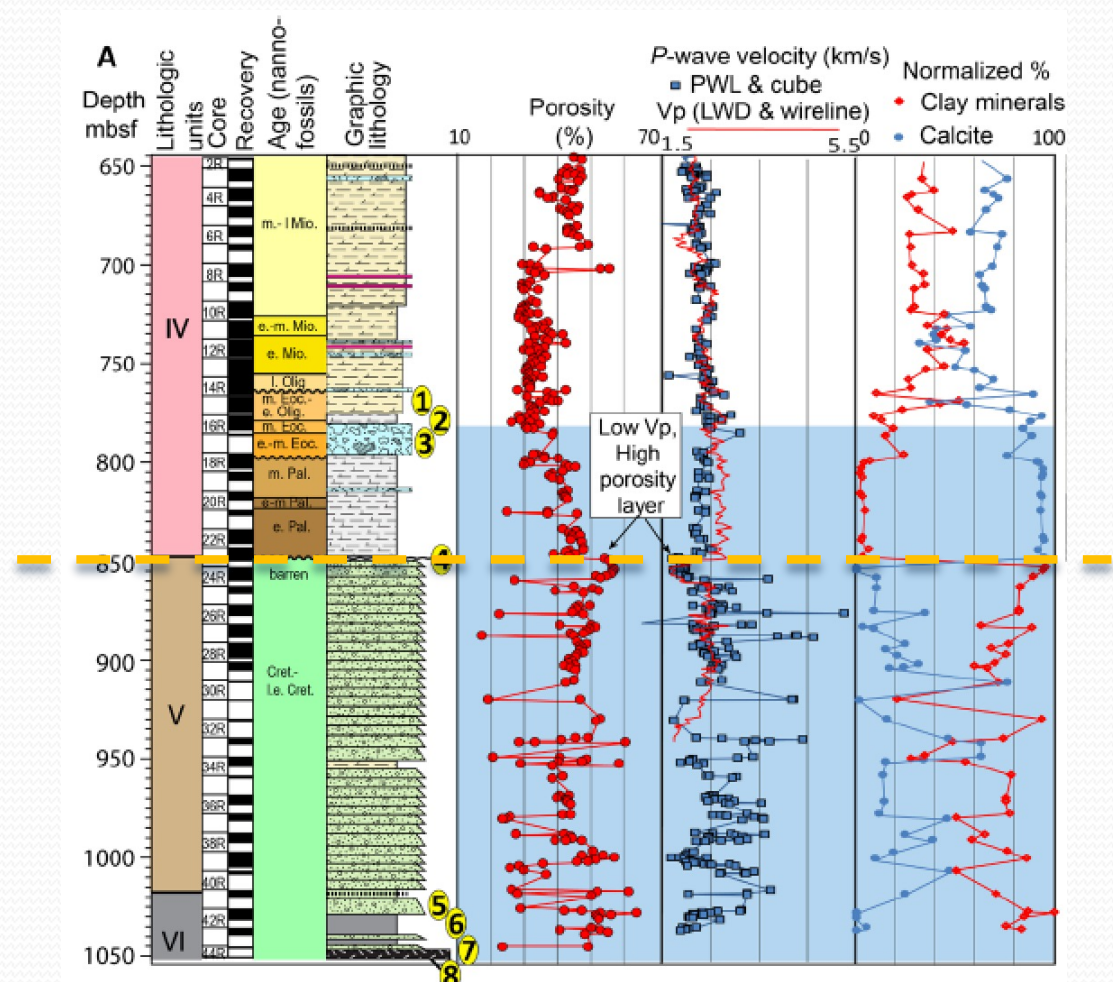
Blue line is the stratigraphic interval correlated down-dip with the plate interface: corresponds to the protolith interval comprising the carbonatic rocks of Unit IV (marls/chalk LU9,10) and the volcanoclastics of Unit V (LU11)



# Core-log-seismic integration

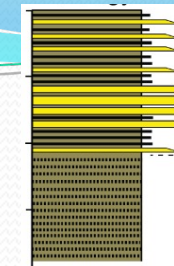
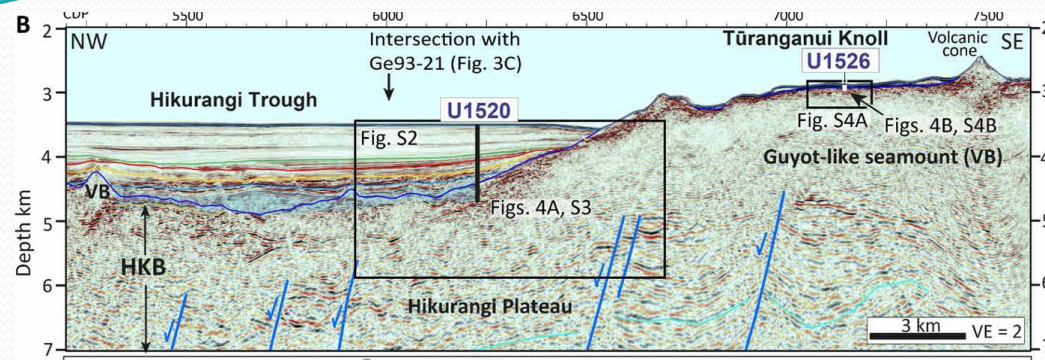
*The control of the lower plate structure on the future plate interface:*

- The transition from the pelagic Unit IV to the volcanoclastics Unit V is associated to a change in most physical properties.
- The mixed volcanoclastic-dominated assemblage comprising units V and VI (i.e. the upper portion of the Hikurangi Plateau) is characterized by highly heterogeneous physical properties: this variability reflects the highly heterogeneous texture, composition, alteration, and cementation of the conglomerate.

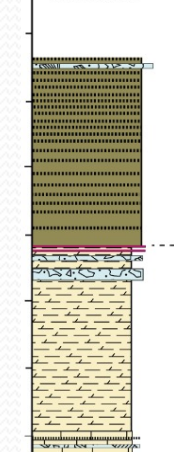
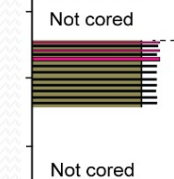


*Barnes et al., 2020, Science Adv.*

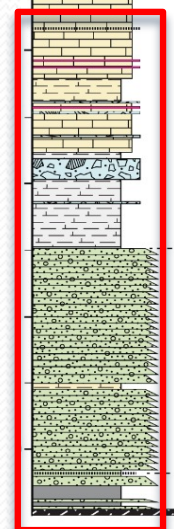
# Summary: what enters the system



U1520



U1526

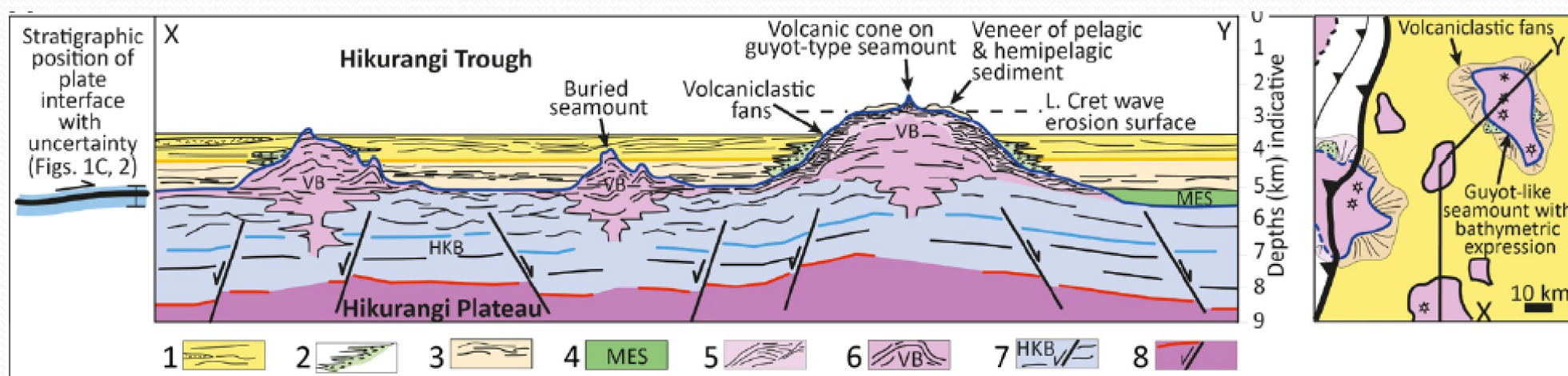


- Highly heterogeneous assemblage of lithologies (turbiditic mud, calcareous marl, calcareous ooze, chalk, MTD, volcanoclastic sands and conglomerate and basalt), with widely varying physical properties, and rough topography.
- Heterogeneity of grain size, sorting and cementation in volcanoclastics are identified.
- Plate interface seems to project to a stratigraphic interval comprising mainly carbonates and volcanoclastic sediments (widely altered to smectite clay) and basalt.
- Lithologies in U1526 can correspond to that at the bottom of U1520.
- The volcanoclastic-dominated interval is not typical of all subduction zones but may be a common feature where seamounts and ridges are subducting.

# Summary: what enters the system

Barnes et al., Science Adv., 2020

## Possible stratigraphic architecture of the subducting plateau



The rough subducting topography contribute to the wide range of lithological assemblages on the incoming plate approaching the subduction system.

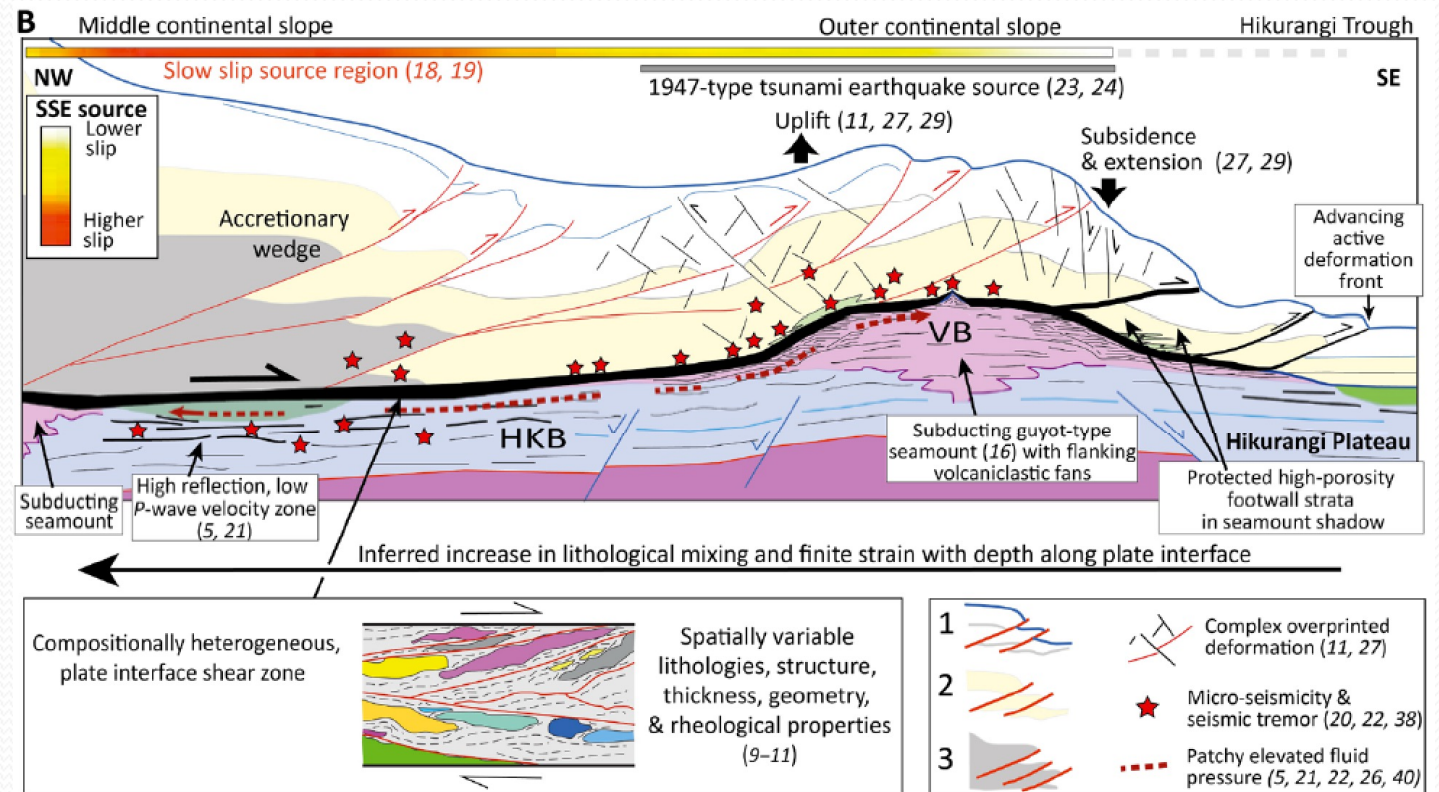
# Summary

## Possible evolution of knoll subduction and seismic character

Different lithological mixing may occur during deformation across the plate interface leading to a fault zone with a highly variable suite of rocks and marked variations in cohesion, elastic moduli, strength, and inferred frictional behaviour

+

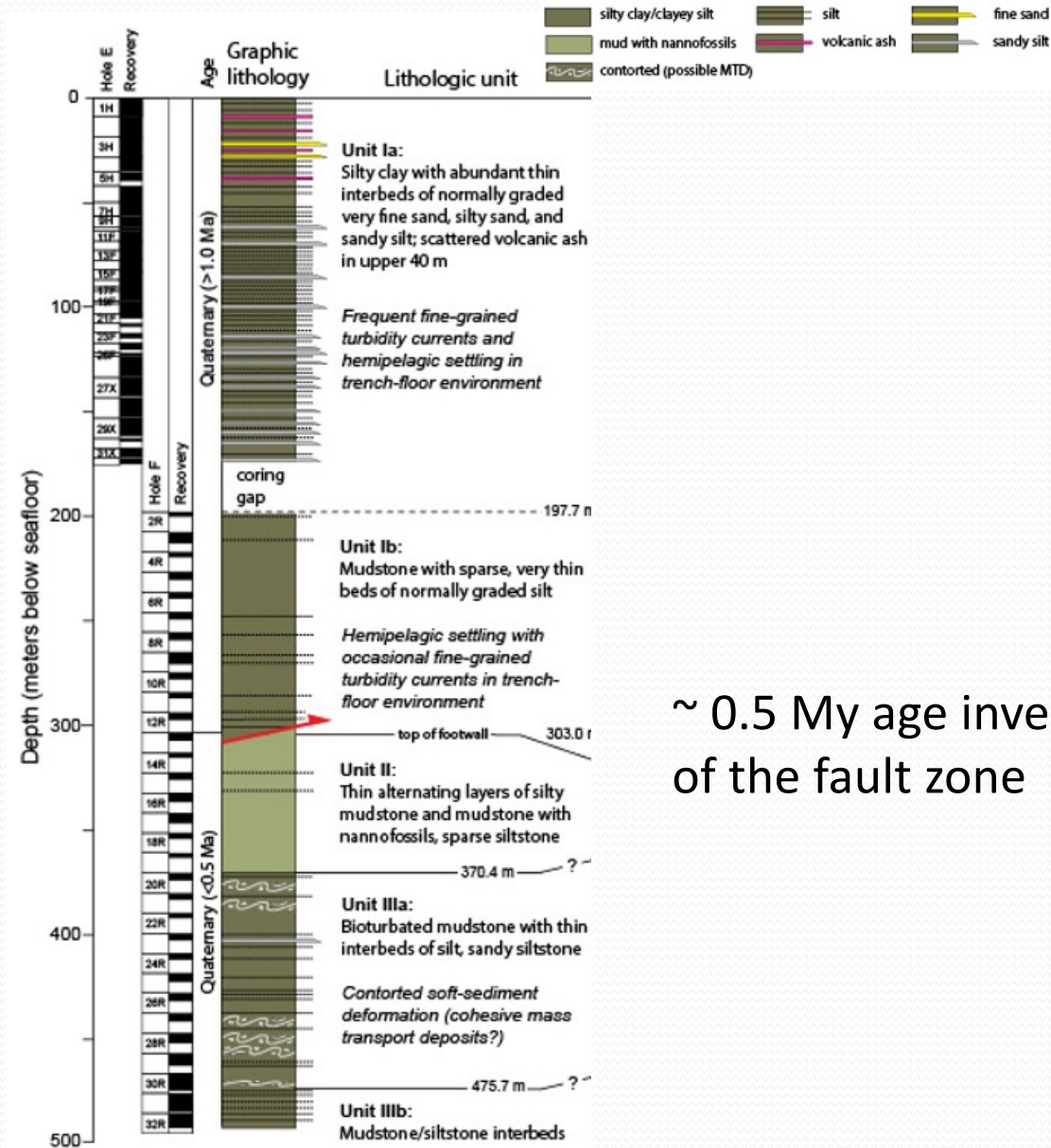
Geodetic and seismological data indicate enigmatic co-existence of patchy (and overlapping) seismic and aseismic slip behavior at Hikurangi



Geometrically irregular fault zone with variable thickness and strain distribution, and comprising a mosaic of diverse lithologies with markedly different mechanical properties **may promote different slip behavior (?)**



# U1518: the Pāpaku shallow thrust



~ 0.5 My age inversion at top of the fault zone

# U1518: the Pāpaku shallow thrust

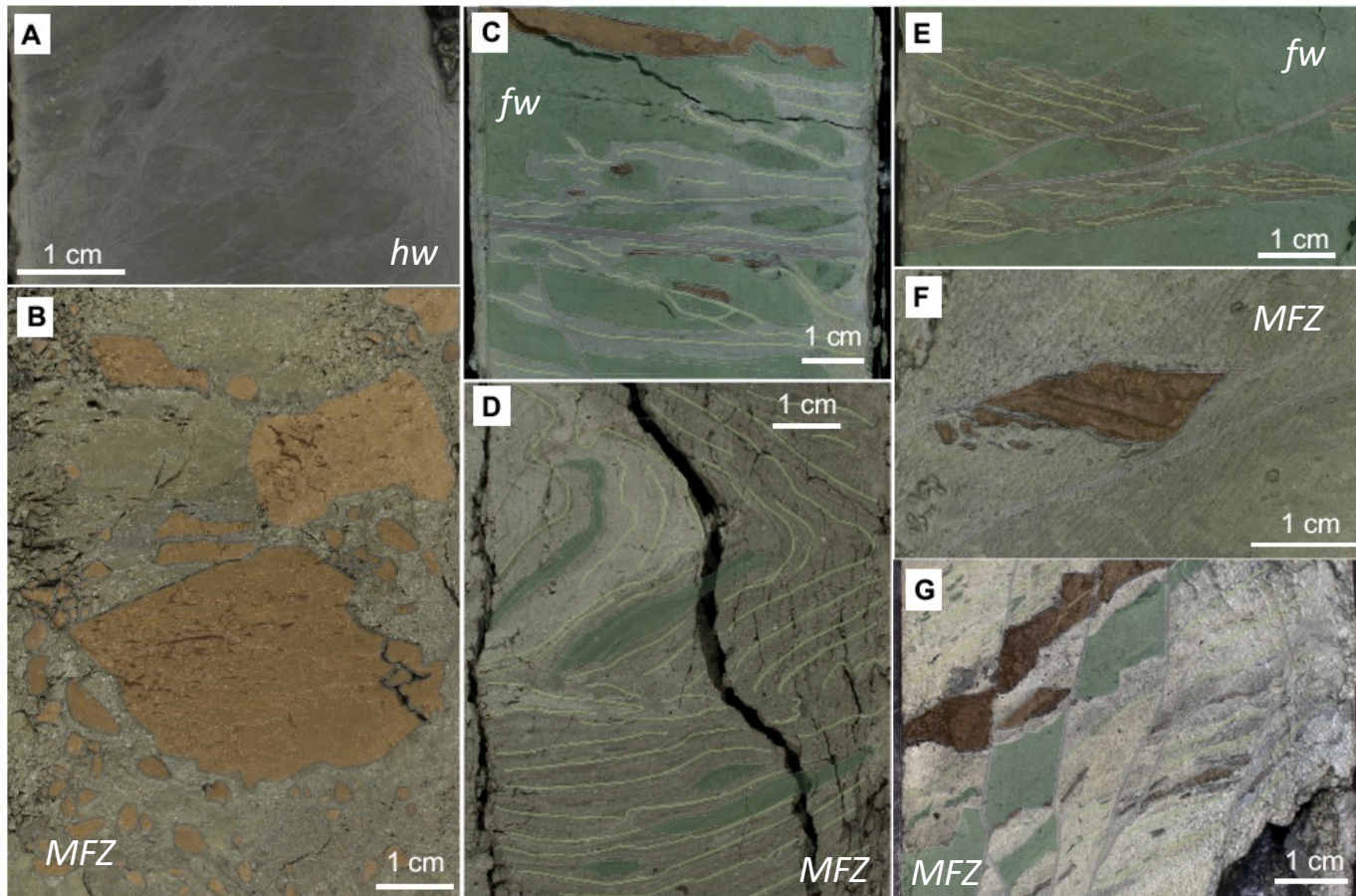
~60-m-thick fault zone with two high-strain zones separated by less-deformed sediments.

HANGING WALL: hemipelagic deposits Early to Mid Pleistocene.

Sets of regularly spaced filled fractures, no evidence of shear. Dominantly rigid compared to the footwall and fault zone. Sharp transition to MFZ

FOOTWALL: bioturbated hemipelagic deposits Mid-Late Pleistocene.

Concentrate most of deformation. Pervasive ductile structures (dismembered beds). Less rigid than HW.



MFZ: Sharp transition to the hanging wall. Lithologically similar to footwall.

Mix of intensely brecciated, fractured, and flow banded, dismembered ductily sheared silt and mud (ca. 18 m thick) Brittle deformation also comprises faults healed by fine clays which crosscut ductile structures.

brittle vs. ductile deformation either cyclic, or brittle deformation progressively became more dominant w/ lithification

# COULD SHALLOW, NORMALLY CREEPING PAPAKU FAULT PROPAGATE A SEISMIC RUPTURE NUCLEATING AT DEPTH?

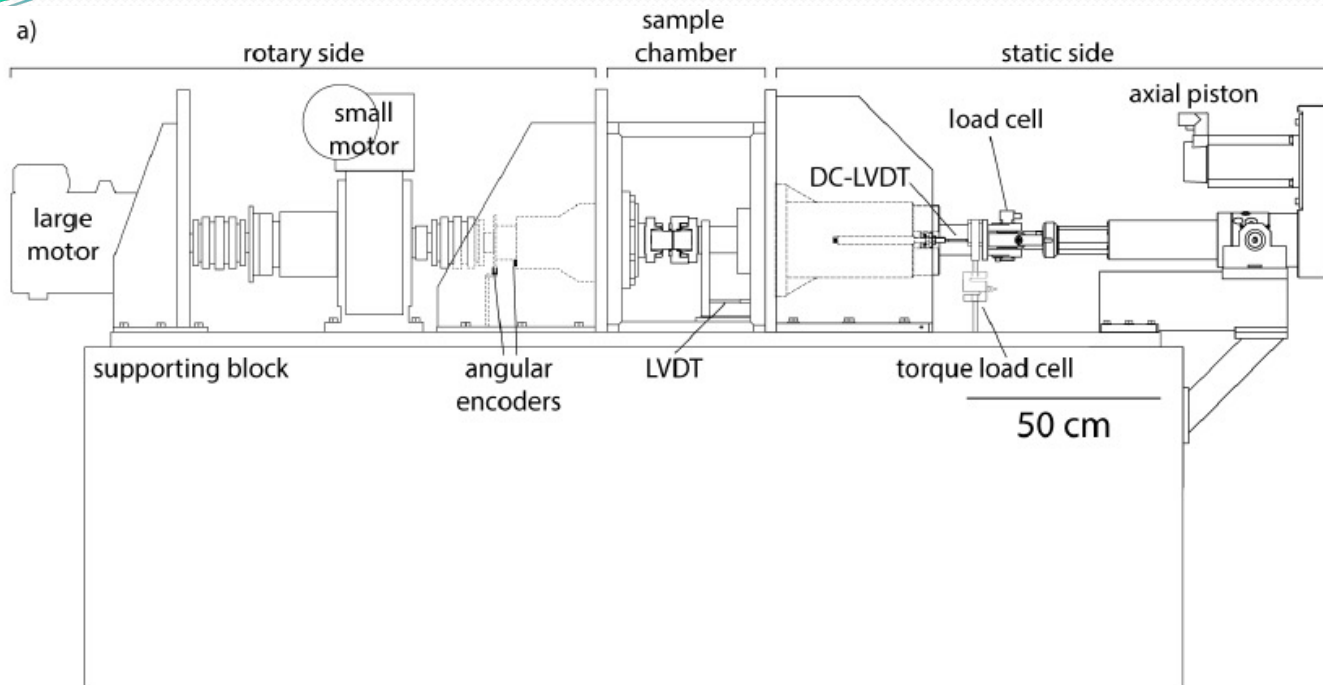
On selected samples from main fault zone, hanging wall and footwall, we performed:

- high velocity friction experiments (SHIVA, INGV, Rome) using an innovative experimental setup allowing fluid saturation and the measurement of pore pressure and temperature.
- Samples: 12R1 (HW, ~9 m above the fault zone ), 14R1A (FC-MFZ), and 21R3 (FW, ~19 m below the fault zone).

All clay-rich sediments with an average mineral composition of:

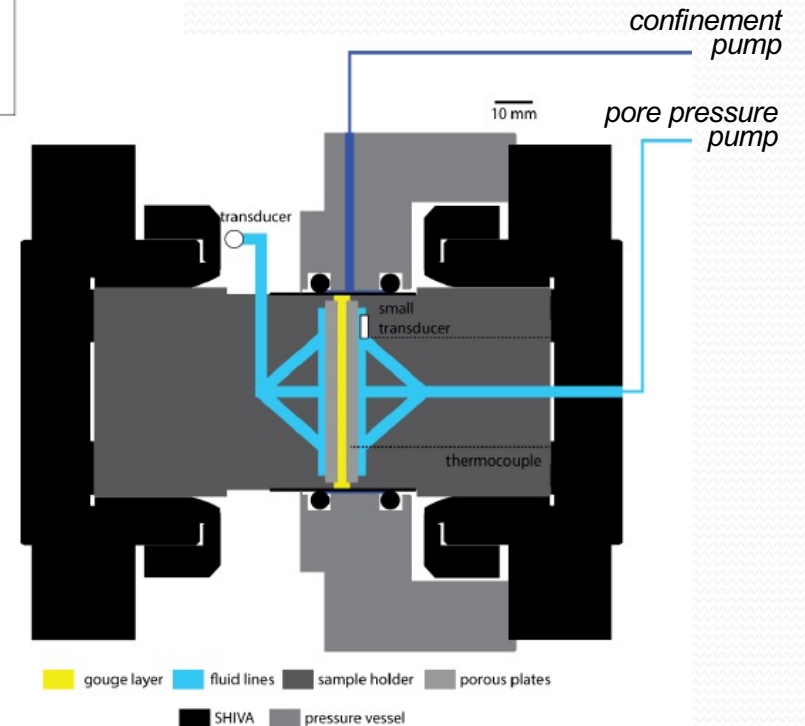
45.4 ± 2.1 wt.% total clay minerals (smectite + illite + chlorite + kaolinite),  
28.7 ± 0.8 wt.% quartz,  
17.2 ± 0.6 wt.% feldspars,  
10.8 ± 0.8 wt.% calcite

# SHIVA (Slow to High Velocity Apparatus) @ INGV, Rome



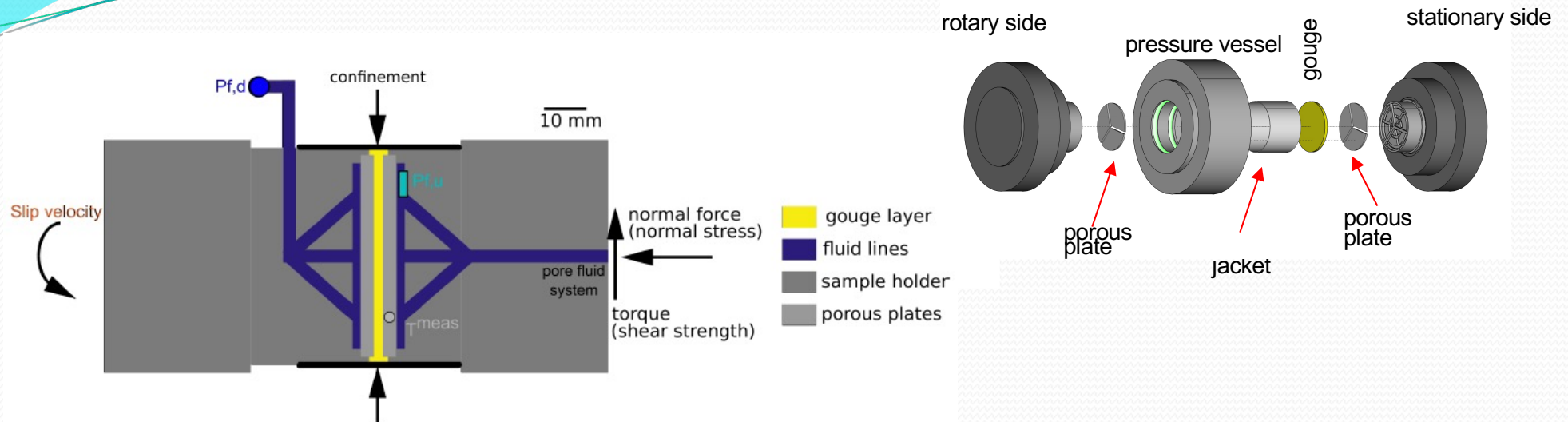
$s_n < 60 \text{ MPa}$   
 $v = 10 \text{ mm/s} - 5 \text{ m/s}$   
 $d = \text{infinite}$   
 Power 300 kW  
 Torque 1100 Nm

(new set up and experiments performed by Dr. Stefano Aretusini and Dr. Elena Spagnuolo)



Sample chamber and sample holder

## The new experimental setup for exp in controlled fluid pressure



- gouge layers (250  $\mu\text{m}$  grain size), ca. 4.5 mm thick, between two sample holders with steel porous plates, and jacketed with a PVC shrink tube.
- the jacketed sample is inserted into a water-filled pressure vessel to provide a confining pressure ( $P_c$ ),
- pore fluid (distilled water) is injected into the gouge layer from the static side and monitored with transducers on the rotational ( $P_{f,d}$  = pressure downstream) and on the static side of the sample ( $P_{f,u}$  = pressure upstream).
- Normally normal stress, axial shortening, displacement, velocity, shear strength (evolution of material strength) are measured. In these experiments we added (i) **pore pressure**, (ii) **temperature at the edge of the gouge layer** with a thermocouple.
- fault gouge was tested without adding water for room humidity conditions. To impose water dampened conditions, deionized water was added to the gouge layer so that it was only partially saturated.

## The new experimental setup for exp in controlled fluid pressure

10 experiments to measure the dynamic evolution of the shear strength :

**6 fluid-pressurized tests** on FC, HW and FW,

-  $S_n = 6$  MPa,  $P_c = 4$  MPa,  $P_f = 3$  MPa

- room temperature (25°C)

- for each experiment, first we gradually increased  $S_n$  and  $P_c$ ,

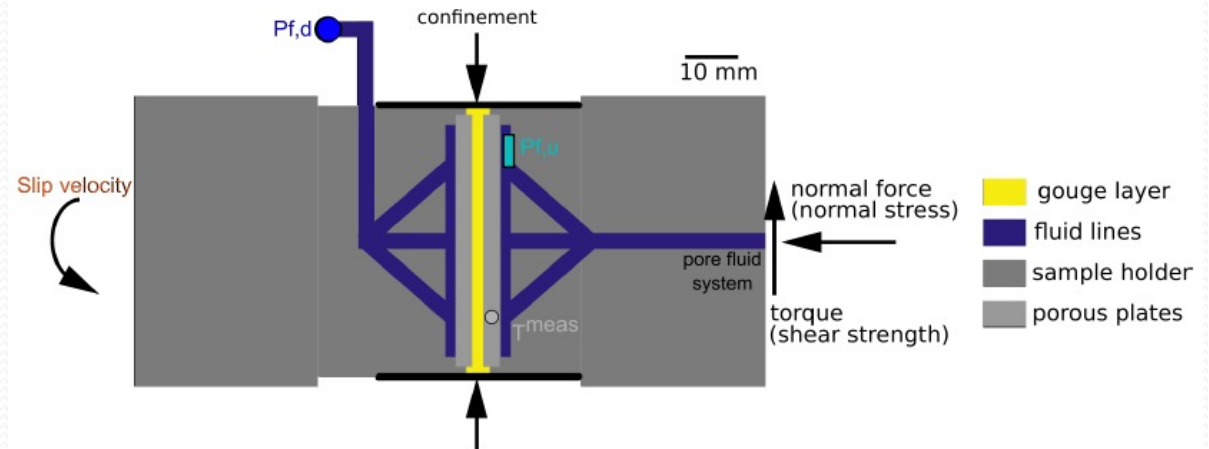
and then  $P_f$

-  $P_f$  is equilibrated between the two sides of the gouge layer before shear pulses to ensure saturation

**4 additional tests** on FC samples under room humidity and water dampened conditions, at room temperature (25° C) and normal stress of 3 MPa (i.e. effective normal stress identical to the pressurised experiments)

Samples: 12R1 (HW), 14R1A (FC), and 21R3 (FW)

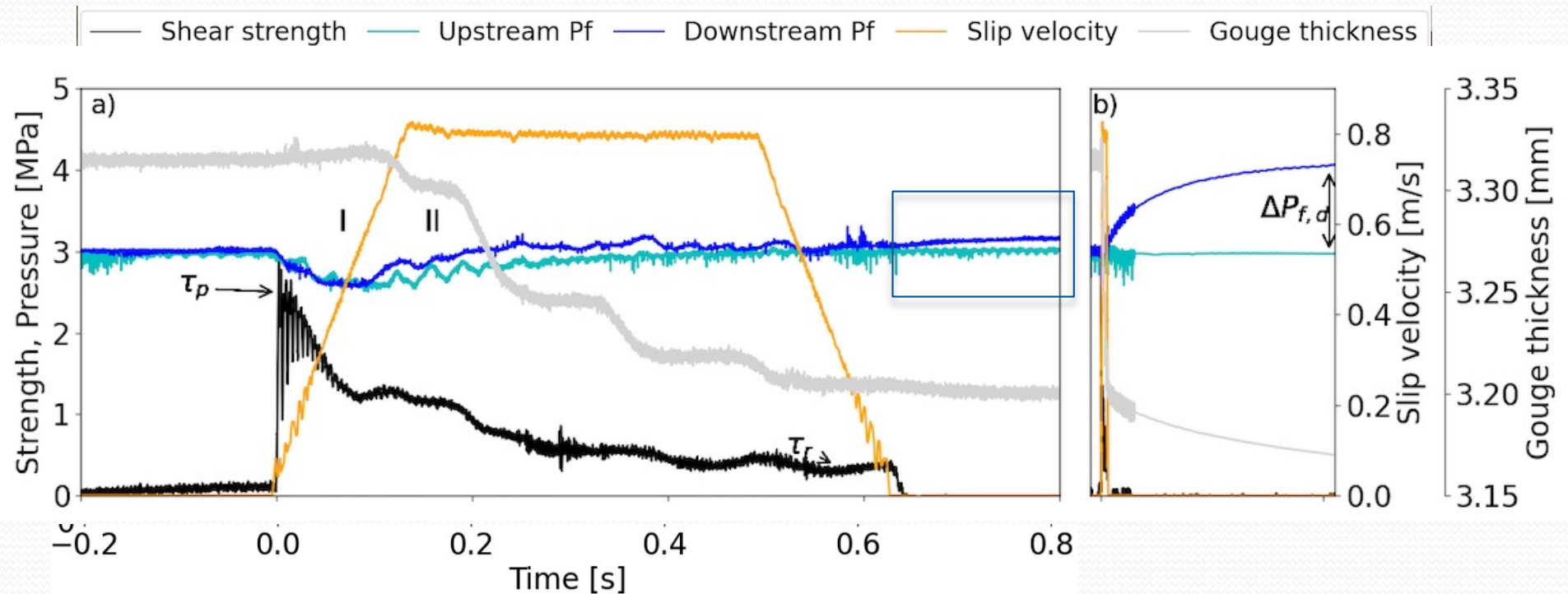
- PRE-SHEAR: slip pulse at 10  $\mu\text{m/s}$  for 0.01 m of slip, to achieve compaction
- after equilibration of pressure FAST SLIP PULSE at 0.8 m/s for 0.4 m of slip (i.e. a moderate (Mw 6.0-6.5) tsunamigenic earthquake)



# Results: mechanical behavior across Pāpaku thrust materials

Aretusini et al., Nat. Comm,  
accepted

## Anatomy of the seismic velocity slip pulse (pressurized test)



Independently of fault material, in all the pressurized experiments  $P_f$  increase in different ways and at different times during/after the fast slip pulses:

- $P_f$  decrease after the onset of slip associated to a **gouge layer thickness increase**
- the maximum downstream increase  $\Delta P_f (= P_{f,d} - P_{f,u})$  accompanied by **gouge layer thickness reduction**
- **shear strength decays is different** in different materials (i.e. different slip weakening distance  $D_w$ )

## Results: mechanical behavior across Pāpaku thrust materials

What do the experiments suggest?

Pāpaku Thrust materials, when sheared at seismic velocities:

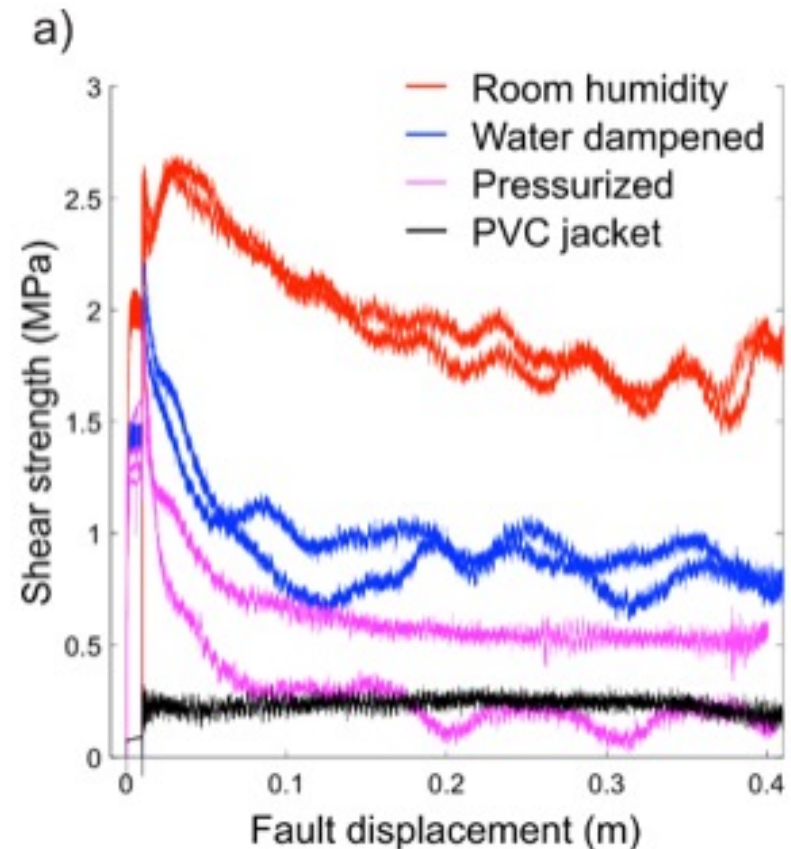
**1) Shear strength decay = DYNAMIC WEAKENING**, in ALL SETS of experiments

(depends on peak strength, residual strength, and slip weakening distance);

In pressurized experiments

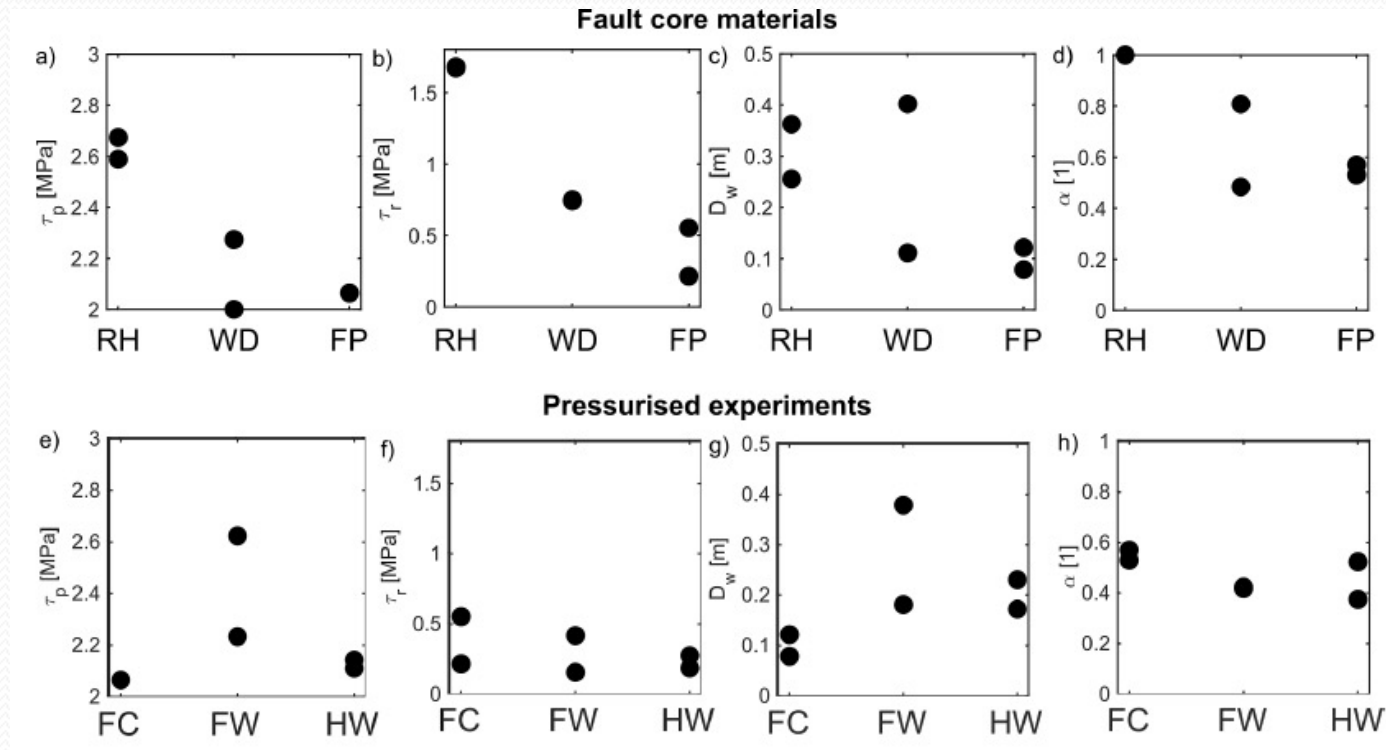
**2) Decrease in pore fluids pressure** at onset of slip and thickening of the gouge layer - possibly suggesting shear enhanced dilatancy?

**3) Pressurization of pore fluids** during/after the slip pulse associated with thickness reduction of the gouge



## Results: mechanical behavior across Pāpaku thrust materials

In particular:



- FC materials showed the **lowest** peak strength ( $\tau_p$ ), residual strength ( $\tau_r$ ), and slip weakening distance ( $D_w$ ) **under fluid pressurised** conditions than under water dampened and room humidity conditions
- In fluid pressurised experiments, FC materials had the **lowest slip weakening distance** with respect to HW and FW materials.

## ***Dynamic weakening and pressurization***

Several mechanisms can account for pore fluid pressure increase, decrease in shear strength and effective normal stress (see *Aretusini et al., Nat.Comm.* for references):

- 1) *thermal pressurisation*, i.e. pressure increase by frictional heating
- 2) *dehydration* (frictional heating causes clay minerals water dissociation),
- 3) *mechanical pressurisation*, i.e. pore fluid pressurises because the pore volume decreases by compaction during shear

**Evolution of temperature across gouge** (in room humidity and water dampened exp.):

The maximum temperature rise at the centre and edge of the gouge layer was calculated with numerical methods to simulate T evolution.

Then the modelled T at the edge of the gouge was compared to the temperature measured during the experiments:

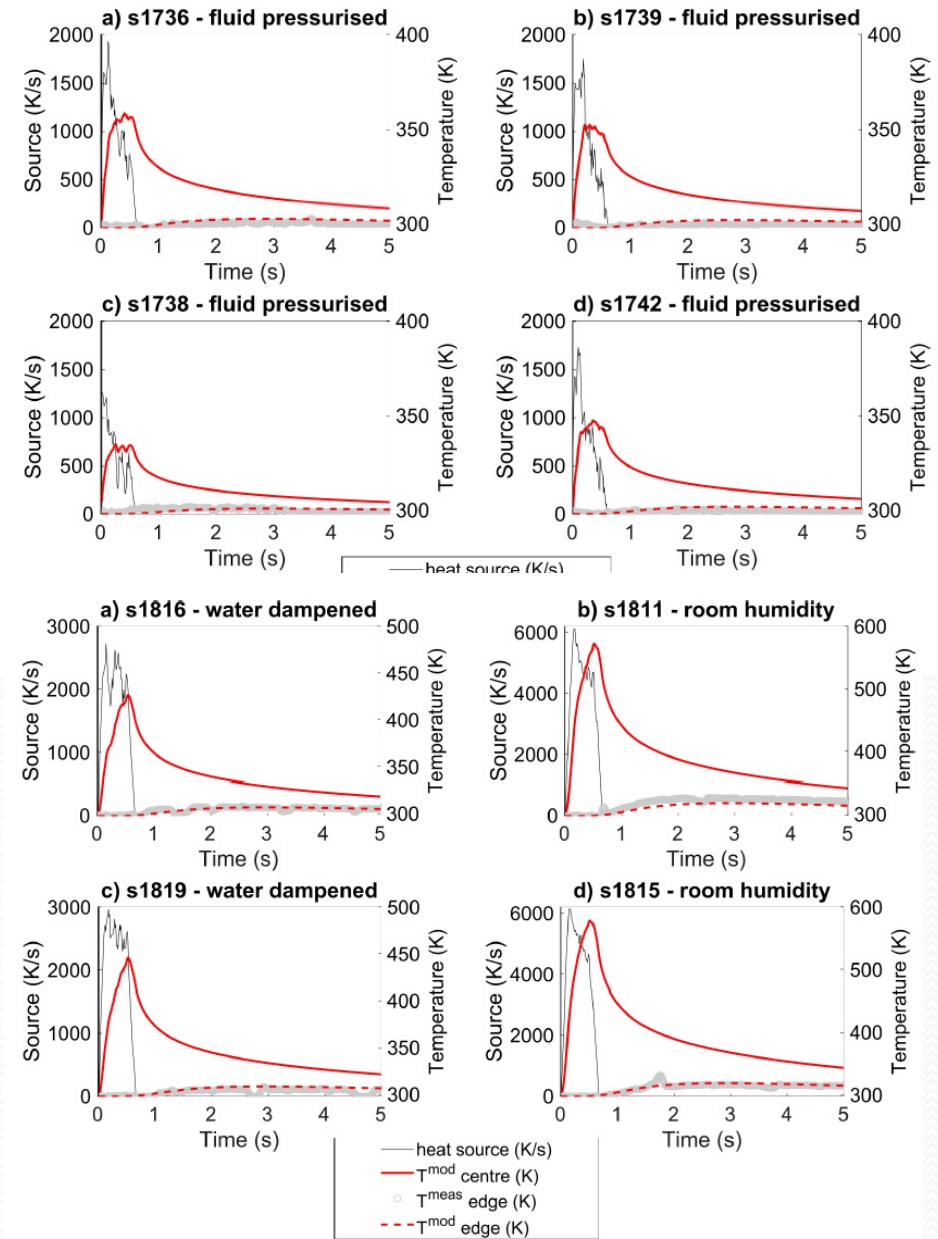
- T measured with the thermocouple was reproduced by the estimated temperature ca. 1 mm away from the gouge layer;
- Therefore, the T modelled at the center of the gouge during seismic slip pulse can be then used to discuss the active pressurization mechanism.

# Dynamic weakening and pressurization

## Estimated maximum temperature and pressurization mechanisms

In the room humidity experiments, the absence of water and the **highest estimated maximum temperature** suggest that dehydration and/or a thermally- activated processes are dominant in governing dynamic weakening.

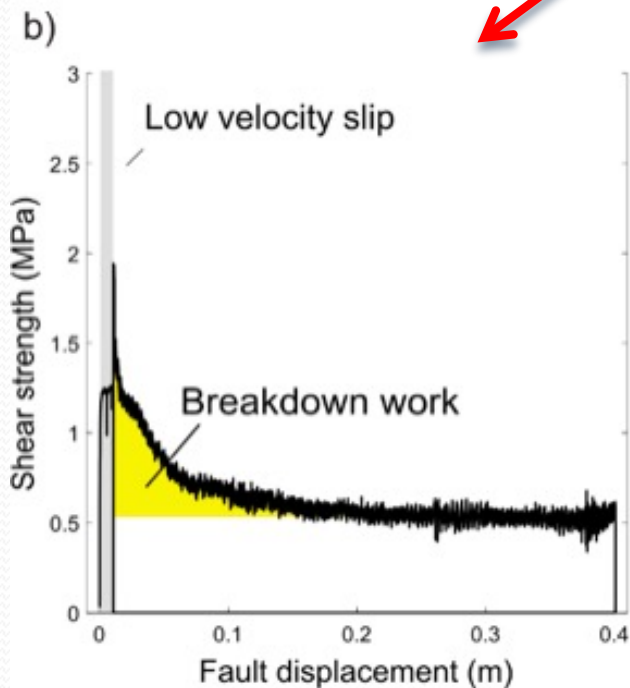
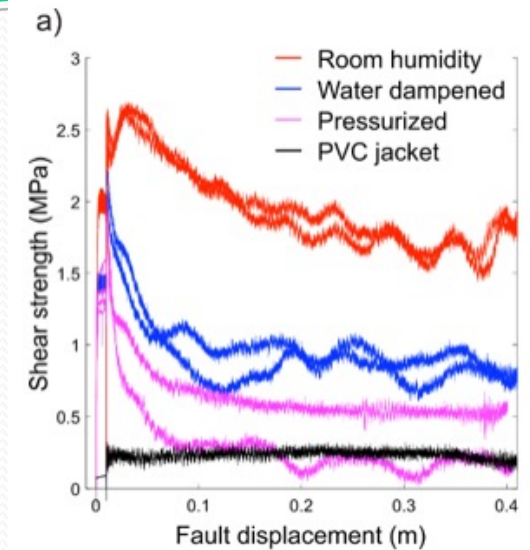
In presence of pore fluids, dynamic weakening is associated with **pore fluid pressure increase**, and the **estimated maximum temperature** in the centre of the slipping zone is lower.



A combination of thermal pressurisation, dehydration and shear compaction drove the pore fluid pressure increase and therefore the shear strength reduction.

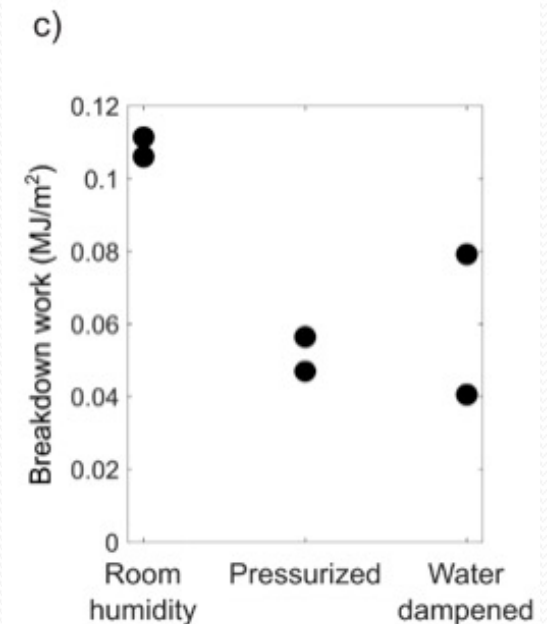
## Estimation of the breakdown work

$W_b$  = energy dissipated during the loss of strength.  
Calculated from the shear strength variation with displacement, it controls earthquake rupture propagation: smaller  $W_b$ , increasing ease of rupture propagation.  
Depends also on slip weakening distance  $D_w$



FC materials under fluid pressurised conditions have the lowest residual stress and smallest slip weakening distance;

Pāpaku thrust FC materials have the lowest  $W_b$  when deformed under fluid pressurized or water dampened conditions with respect to tests at room humidity.



## Take away messages

- **Pressurization** with seismic slip at 0.8 m/s is observed in fault core and damage zones, associated with **dynamic weakening**
- The presence of liquid water activates fluid-driven processes which reduce the energy required to propagate seismic rupture  $W_b$  more efficiently than thermally-driven processes activated under room humidity conditions.
- The lower  $W_b$  in fluid-pressurised conditions can be explained by the faster initial dynamic weakening and shorter  $D_w$  than in the other environmental conditions.

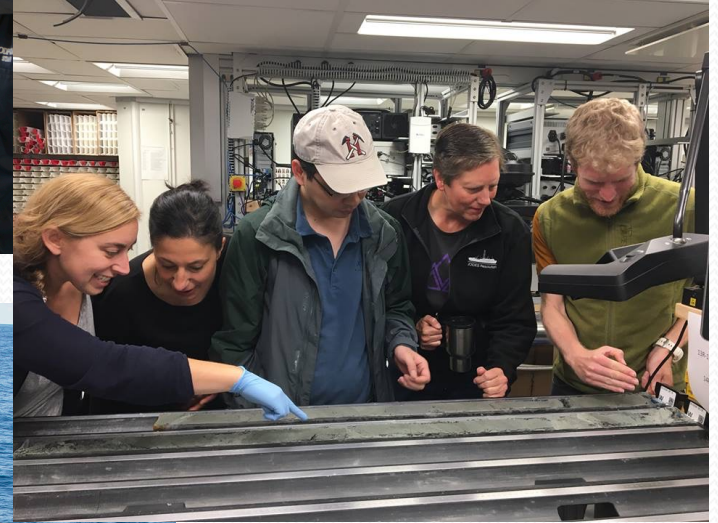


**The coseismic mechanical pressurisation of fluids (enhanced by the low permeability of the fault), reduces the energy required to propagate upward an earthquake rupture**  
**Fluid-pressurised faults are demonstrably prone to seismic slip if perturbed by arrival of a seismic rupture, i.e. when activated, Pāpaku splay can propagate slip easily up to the trench.**

- Fault core have lower  $W_b$  compared with HW and FW (shorter  $D_w$ ).



**Seismic slip at shallow depths can propagate in any of these materials and/or FC materials at Pāpaku fault can be the slightly most favourable to propagate fault slip if perturbed by a seismic rupture**



**GRAZIE!**